44th AIAA/ASME/SAE/ASEE Joint Propulsion Conference
20-23 July, 2008, Hartford, CT
AIAA-2008-4917

Dawn Ion Propulsion System – Initial Checkout after Launch

John R. Brophy[1], Charles E. Garner[2], and Steven Mikes[3]
Jet Propulsion Laboratory, California Institute of Technology, Pasadena, CA 91109

The first 80 days after launch of the Dawn mission were dedicated to the checkout of the spacecraft with a major emphasis on the ion propulsion system. All three ion thrusters, all three thruster-gimbal assemblies, both power processor units, both digital interface & control units, and the entire xenon feed system were completely checked out and every component was found to be in good health. Direct thrust measurements agreed well with preflight expected values for all three thrusters over the entire throttle range. Measurements of the thruster-produced roll-torque verified that each thruster produces less than the maximum allowed value of 60 μNm at full power. Thruster electrical operating parameters and power processor units efficiencies also agreed well with preflight expected values based on acceptance test data. Two of the three ion thrusters were fully checked out within 30 days after launch. Checkout of all three thrusters was completed 64 days after launch. Deterministic thrusting with the IPS began on December 17, 2007

I. Introduction

The Dawn spacecraft was launched on September 27, 2007 in the early morning, shortly after dawn. The first 80 days after launch were dedicated to a thorough checkout of the spacecraft. A principle focus of this checkout activity was the ion propulsion system (IPS). Proper functioning of the IPS is critical to the success of the mission. The IPS is required to provide all of the post-launch ΔV (aside from the Mars gravity assist) including the heliocentric transfer to Vesta, orbit capture at Vesta, transfer between science orbits at Vesta, escape from Vesta, heliocentric transfer to Ceres, orbit capture at Ceres, and transfer between science orbits at Ceres. To accomplish this the ion propulsion system must provide a total ΔV of approximately 10.6 km/s to the spacecraft which had an initial wet mass of 1218 kg including 425 kg of xenon and 46 kg of hydrazine. Additional details of the mission and spacecraft are given elsewhere [1-4].

A simplified block diagram of the Dawn IPS is given in Fig. 1. The ion propulsion system includes three 30-cm diameter xenon ion thrusters of the type flown on DS1 [5-8], two power processor units (PPUs), and two digital control & interface units (DCIUs). The IPS has a light-weight, composite xenon tank developed specifically for Dawn which can store up to 425 kg of xenon. In addition to the xenon tank, the xenon feed system includes two plenum tanks, a xenon control assembly (XCA), a high-pressure subassembly, nine service valves, the interconnecting tubing, and nine flexible propellant lines that go across the gimbal interfaces. Finally, the IPS includes three, 2-axis thruster-gimbal assemblies (TGAs). Each TGA provides two-axis thrust vector control with a capability of approximately ±8 degrees in one axis and ±12 degrees in the other.

The xenon feed system, described in Ref. 9, controls the pressure in each plenum tank to control the flow rate to each thruster. The pressure is controlled using a bang-bang regulation system that cycles the high-pressure solenoid valves in response to the difference between the measured plenum pressures and the required pressure.

[1]Section Staff, Propulsion and Materials Engineering Section, Member AIAA
[2]Member of the Technical Staff, Propulsion and Flight Systems Group
[3]Member of the Technical Staff, Electronic Design Group

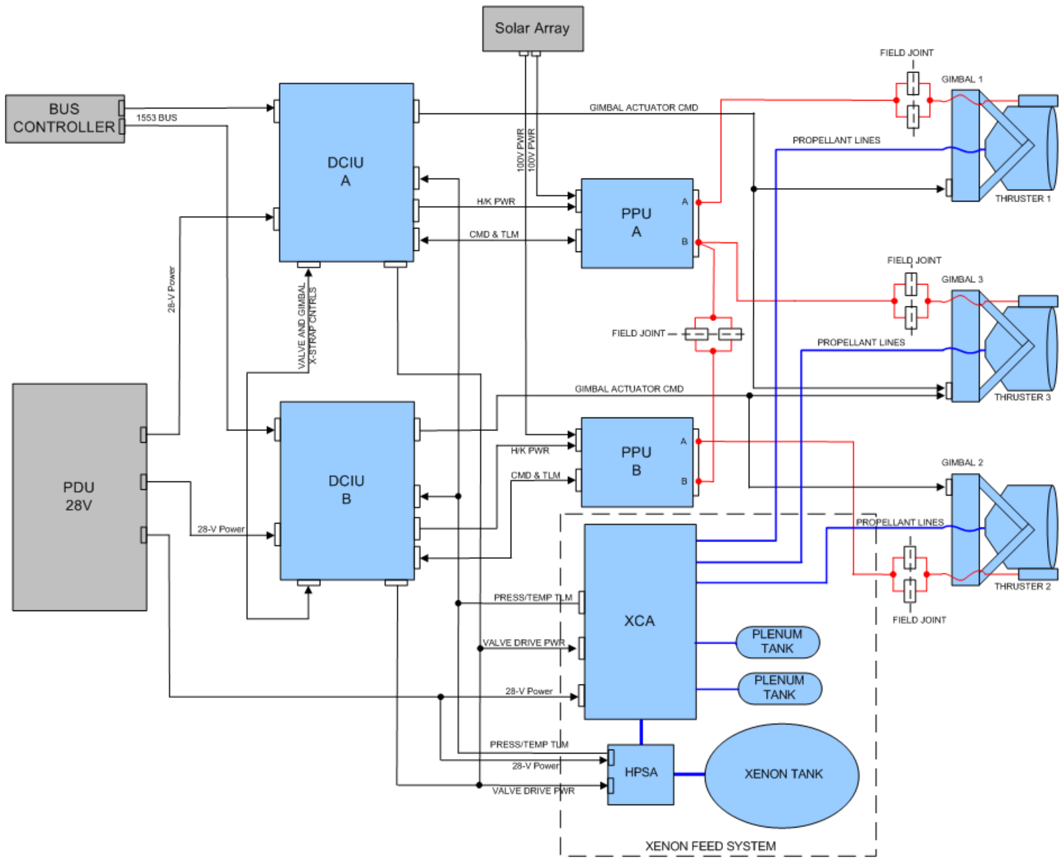

Fig. 1. Simplified IPS block diagram.

The Dawn ion propulsion system is designed to be single-fault-tolerant. To accomplish the mission at least two ion thrusters, two TGAs, one PPU, and one DCIU must be fully functional after launch. During the 80-day checkout period the functionality of all of the IPS hardware was tested and the results are summarized below. A list of the key IPS-related checkout activities is given in Table 1. Operation of the IPS during normal cruise, which began on December 17, 2007, is described by Garner [10].

II. IPS Preparation Activities

After launch, several activities were performed to prepare the ion propulsion system for operation. These activities began at launch plus four days with the bake-out of the propellant lines downstream of the flow control devices in the XCA followed by cathode conditioning, pressurization of the plenum tanks, initialization of each TGA, cathode ignition and operation of each thruster in diode-mode for two hours. The checkout plan identified FT3 as the first thruster to be tested. This thruster can be operated by either PPU, is referred to as the "shared" thruster, and is physically located in the center position as indicated in Fig. 2. Thruster FT2 is on the sun-side of the spacecraft positioned below the high-gain antenna, and FT1 is on the shade-side of the spacecraft.

The plan called for FT3 to be operated from PPU-1 during the ICO phase. Each PPU has relays that switch its outputs between each of two thrusters. The relays in the PPU-2 can be in any state when the shared thruster FT3 is operated by PPU-1, but it is preferred that they be set such that their outputs are switched to FT2. To reinforce the desired state of the relays in PPU-2 after launch, the first activity for the IPS was to turn on DCIU-2 and PPU-2, and command the relays to FT2. This activity also provided early insight to the state of health of DCIU-2, PPU-2, and the XFS. All of the telemetry from DCIU-2 indicated that both it and PPU-2 were functioning normally, that DCIU-2 was correctly reading all of the analog signals from the XFS, and that the xenon tank and plenum tank pressures were as expected (i.e., still at the values set prior to launch).

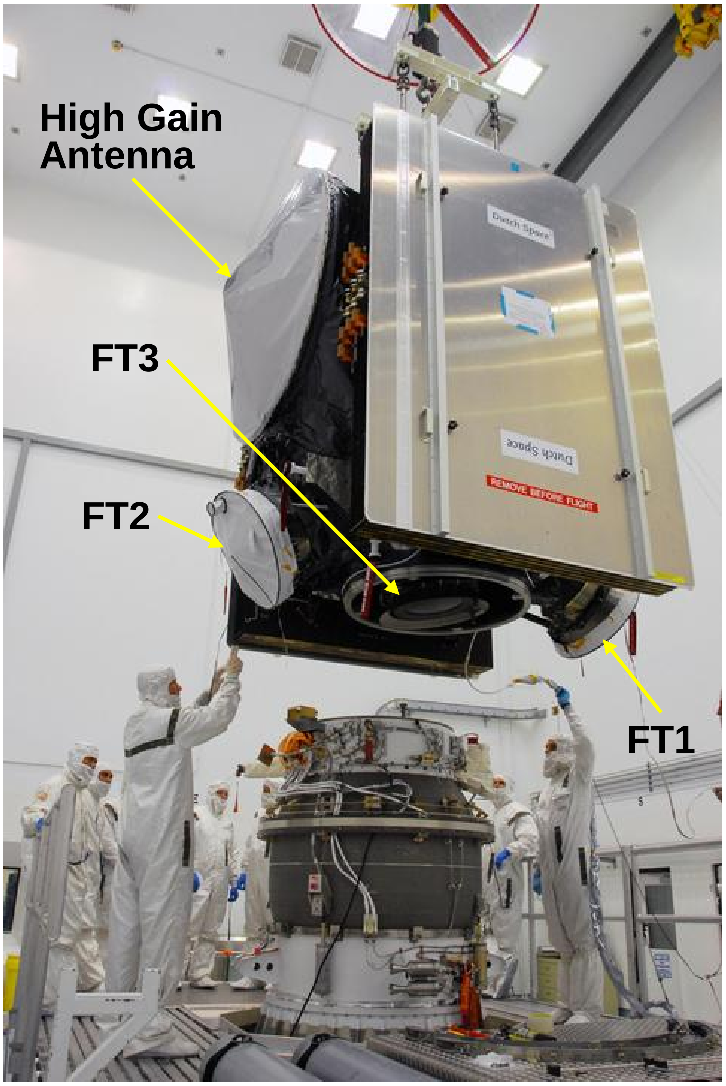

Fig. 2. The Dawn spacecraft showing the locations of the three ion thrusters in the IPS.

The next activity was the propellant line bake-out which was successfully completed without incident. Cathode conditioning was performed on each thruster prior to the initial cathode ignition. Cathode conditioning is used to bake absorbed water from the cathode emitters the procedure followed the same cathode conditioning process used on DS1 [8] and in each of the key long-duration thruster life tests [11,12]. PPU-1 was used for the cathode conditioning of both FT1 and FT3, while PPU-2 was used for FT2. The cathode heater currents and voltages for all six cathodes (two in each thruster) were as expected.

Initialization activities for the XFS and TGAs were performed prior to cathode ignition and thruster operation in diode-mode. The XFS initialization pressurized the plenum tanks from their launch pressures to the pressures required for thruster startup. Prior to launch the pressures in the plenum tanks were set such that there was a pressure difference between the tanks. After launch IPS telemetry confirmed that there was no change in the pressure of either plenum tank indicating that none of the normally-closed latch valves leaked or changed state during launch. Initialization of the TGAs began with the confirmation that each thruster-gimbal assembly had not moved from its launch position during launch. Each TGA was then driven to its neutral position in preparation for thruster operation. All three TGAs were found to be in good health and performed as expected.

The final preparation activity before operation with beam extraction was to bake-out each thruster by operating it in diode-mode for two hours. Diode-mode operation requires the xenon feed system to provide main, cathode, and neutralizer flow rates at the correct levels and subsequent ignition of both neutralizer and discharge cathodes. Prior to launch the cathodes were purged with dry nitrogen almost continuously from the time they were first assembled. At certain times during the spacecraft assembly and test process, however, it was not possible to purge the cathodes. The total time off purge at the time of launch for the cathodes in each of the Dawn ion thrusters is given in Table 2. This slightly exceeded the maximum allowable time off purge of 1200 hrs. Since the absorption of water by the cathode emitters is known to be a self-limiting process, this was considered to be low risk. Ignition of the cathodes is essential to the operation of the ion thrusters and its successful demonstration after launch represented a major milestone in the checkout activities.

Table 2. Off Pure Times.

Thruster	**Time Off Purge (hrs)**
FT1	1231
FT2	1120
FT3	1087

FT3 was the first thruster to be started. The neutralizer cathode was successfully started 21 seconds after the completion of the 6-minute preheat time. The discharge cathode started immediately upon application of the start voltage. The thruster was then operated in diode-mode for approximately two hours. The second thruster to be started was FT1. The neutralizer and discharge cathodes for FT1 both started immediately after the 6-minute preheat. The thruster was subsequently operated in diode-mode for two hours. FT2 was the final thruster to be started. Again, both the neutralizer and discharge cathodes for FT2 started immediately after the 6-minute preheat. This thruster is located on the +X, sun-side of the spacecraft. Thermal concerns limited the diode-mode bake-out duration to only 20 minutes for FT2. This was necessary to make sure that no fault-protection temperature limits for the thruster were exceeded during this bake-out for the given sun angle. Diode-mode operation of FT2 was successfully completed. The shorter diode-mode bake-out for FT2 was not considered to be an issue since the thruster was more than adequately baked-out by virtue of it being heated by the sun for weeks prior to its first operation.

III. Thruster Checkout

A key objective of the overall spacecraft checkout activity was to determine the health and performance of each of the three ion thrusters in the IPS. The Dawn ion thrusters are designed to operate over the range of PPU input powers from 510 W to 2550 W. This power range is divided into 112 different throttle levels referred to as mission levels, abbreviated ML, ranging from ML0 for the lowest power to ML111 for full power as shown in Table 3. The planned checkout of the ion thrusters called for operating at five different mission levels – ML27, ML48, ML69, ML90, and ML111 – ranging in PPU input powers from 950 W to 2510 W. Electrical parameters, thrust, and the roll torque produced by each thruster were measured at each of these five throttle levels.

During the entire checkout activity a total of 3 kg of xenon was processed by the IPS: 0.40 kg by FT1, 0.22 kg by FT2, and 2.38 kg by FT3. This xenon was processed in approximately 285 hours of IPS operation.

FT3 Performance Characterization

The center thruster, FT3, was started on DOY 2007-280, ten days after launch. After the 6-minute cathode pre-heat both cathodes lit immediately upon application of the start voltages and the thruster was successfully started at ML27. FT3 was then operated at ML27 for the next 11 hours. The first 7 of these 11 hours were used to bleed the plenum tanks in the xenon feed system down to the correct flow rates for ML27 operation. The last four hours at ML27 were used to obtain good thrust measurements. After 11 hours at ML27 the thruster was throttled to ML48 where it was operated for 4 hours, followed by 4 hours at ML69 and 4 hours at ML90. Finally the thruster was throttled to ML111 where it was planned to be operated for 4 hours. However, operation at this throttle level had to be cut short due to thermal concerns elsewhere on the spacecraft unrelated to the IPS. The actual time at ML111 was approximately 1 hour. In this performance characterization test series FT3 was operated continuously for 25 hrs. Steady-state thruster and PPU temperatures were achieved at each throttle level except for the shortened test at ML111.

The measured performance data for FT3 over the 25-hr characterization test are given in Fig. 3. The five different throttle levels are indicated in the top chart in this figure. The vertical lines in this figure indicate high-voltage recycle events. There were 20 high voltage recycles in the first hour after the application of high voltage, six in the second hour, and one in the third hour. Over the full 25-hr test there were a total of 85 high-voltage recycles. In the 65 hours of thruster acceptance testing on the ground there were a total of only 43 high voltage recycles. The higher initial recycle rate after launch is indicative of particulate contamination of the thruster during the spacecraft assembly, test, and launch operations (ATLO). The recycle rate decreased with thruster operating time as the high-voltage arcing eliminated the particulate contamination. The long-duration system test described later, in which FT3 was operated continuously at ML111 for 165.7 hrs had an average high-voltage recycle rate of 1.5 recycles/day. During normal thrusting-cruise at ML111 this rate dropped to ~1 recycle every 3 days [10].

The thruster electrical performance from the in-flight characterization test is compared to that from the thruster acceptance test performed at the test facility of the thruster vendor (L3 Communications, ETI) in Table 4. In this table “actual” refers to the in-flight data, and “expected” refers to the ground-base thruster acceptance test data. These data indicate that the thruster operation in-flight is very similar to that observed on the ground. Also given in Table is the PPU efficiency at each throttle level. It is clear that the PPU is also performing as expected in flight. Measured thrust levels are given in a subsequent section.

Thrust vector control of the spacecraft with FT3 was initiated within three minutes after the thruster was first started at ML27. This was done to minimize the build-up of momentum in the reaction wheel assemblies (RWAs). In thrust vector control mode, the ion thruster provides pitch and yaw control of the spacecraft, with the RWAs providing roll control. The attitude control system was designed to minimize the duty cycle of the TGA actuators. The actuators (provided Starsys Inc., Louisville, CO, USA) consist of a two-phase, 45° stepper motor driving a two stage planetary gearbox which drives a standard harmonic drive system with a 100:1 gear reduction. A duty cycle of 100% corresponds to a step rate of 50 steps/second. The actuator duty cycle during thrust vector control was expected to be less than 1%. The actual duty cycle over the 25-hr characterization test of FT3 was 1.2%. The cumulative number of steps over the 25-hr test period is given in Fig. 4. Recall that the characterization test began at lower power (ML27) and proceed to high power ending at ML111. The data in Fig. 4 indicate that the rate of step accumulation decreases with time. This suggests a lower actuator duty cycle is realized at the higher thrust levels. Subsequent tests at ML111 indicated an actuator duty cycle of approximately 0.5%. The TGA actuators were life tested for 18 times the required life assuming a 1% duty cycle over the mission in which the thruster operating time is divided evenly among the three thrusters.

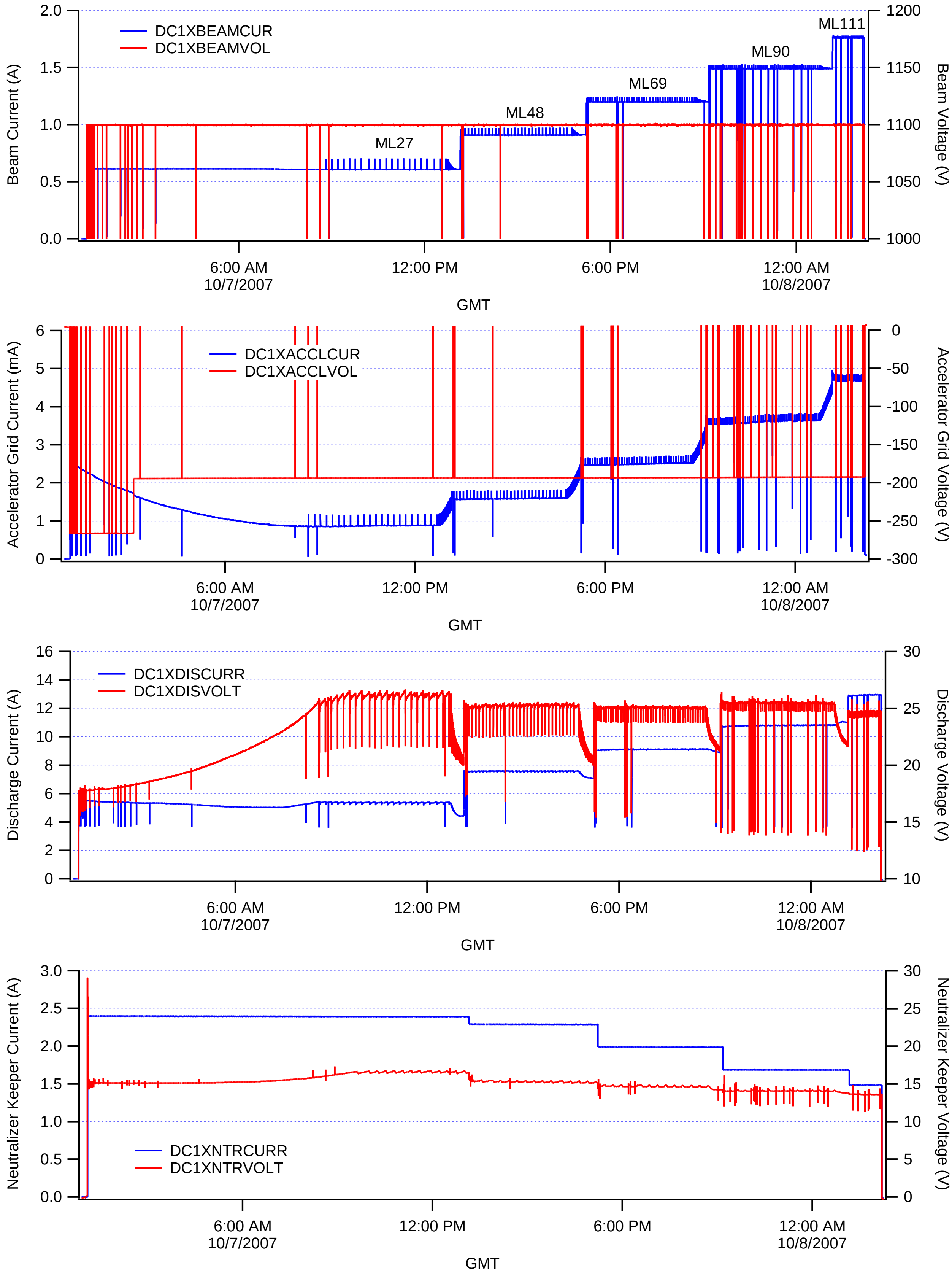

Fig. 3. Electrical parameters from the 25-hr long FT3 characterization test.

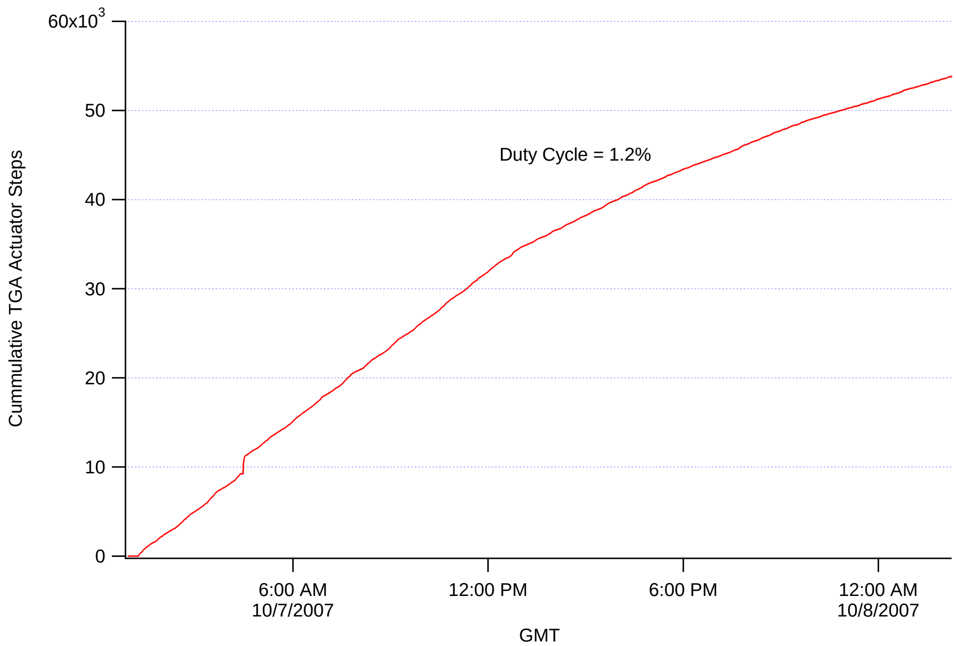

Fig. 4. TGA actuator step in thrust vector control mode during the 25-hr long FT3 characterization test. The actuator duty cycle (slope) is higher in the beginning of the test when the thruster was operated at lower power and thrust.

FT1 Performance Characterization

The cathodes in the outboard thruster, FT1, located on the –X side of the spacecraft were ignited for the first time 13 days after launch for its diode-mode bake-out. The thruster was started with beam extraction for the first time 26 days after launch on DOY 2007-296. After the 6-minute cathode pre-heat both cathodes lit immediately upon application of the start voltages and the thruster was successfully started at ML27. Performance characterization for FT1 followed the same procedure used for FT3 starting with 11 hours of operation at ML27 and stepping up in power through ML28, ML69, ML90, and ending at ML111, with four hours spent at each throttle level. In this performance characterization test series FT1 was operated continuously for 28 hrs, and steady-state thruster and PPU temperatures were achieved at each throttle level.

The key electrical parameters for FT1 over the 28-hr performance characterization test are given in Fig. 5. As before the five different throttle levels are indicated in the top chart in this figure and the vertical lines indicate high-voltage recycle events. The short vertical lines result from small pressure spikes caused by the operation of the bang-bang pressure regulation system. There was only one high voltage recycle in the 11 first hours after the application of high voltage and only 11 over the full 28-hr test. The lower initial recycle rate for FT1 compared to FT3 is a reflection that this thruster accumulated less particulate contamination during ATLO.

The thruster electrical performance from the in-flight characterization test is compared to that from the ground thruster acceptance test in Table 5. These data indicate that the thruster and PPU operation in-flight is very similar to that observed on the ground. Thrust vector control of the spacecraft with FT1 was also initiated within three minutes after the thruster was started at ML27. There were no issues performing thrust vector control with the outboard thruster FT1 even though it is not aligned along the principle axes of the spacecraft. The TGA actuator duty cycle over the 28-hr characterization test of FT1 was 0.9%. The cumulative number of steps over the 28-hr test period is given in Fig. 6. Similar to Fig. 4 the data in Fig. 6 indicate that the rate of step accumulation decreases with time suggesting a decrease in actuator duty cycle with increasing thrust level.

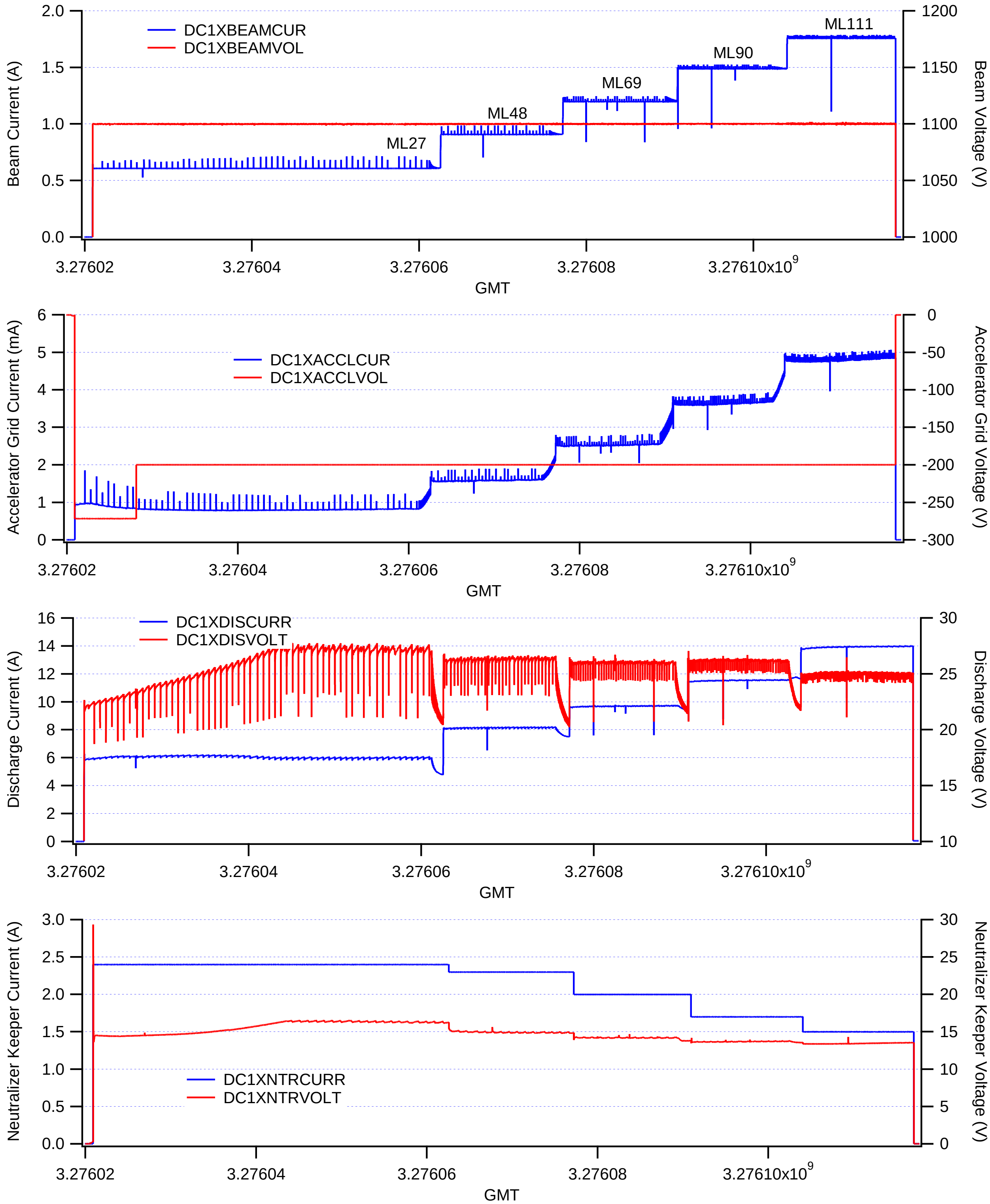

Fig. 5. Electrical parameters from the 28-hr long FT1 characterization test.

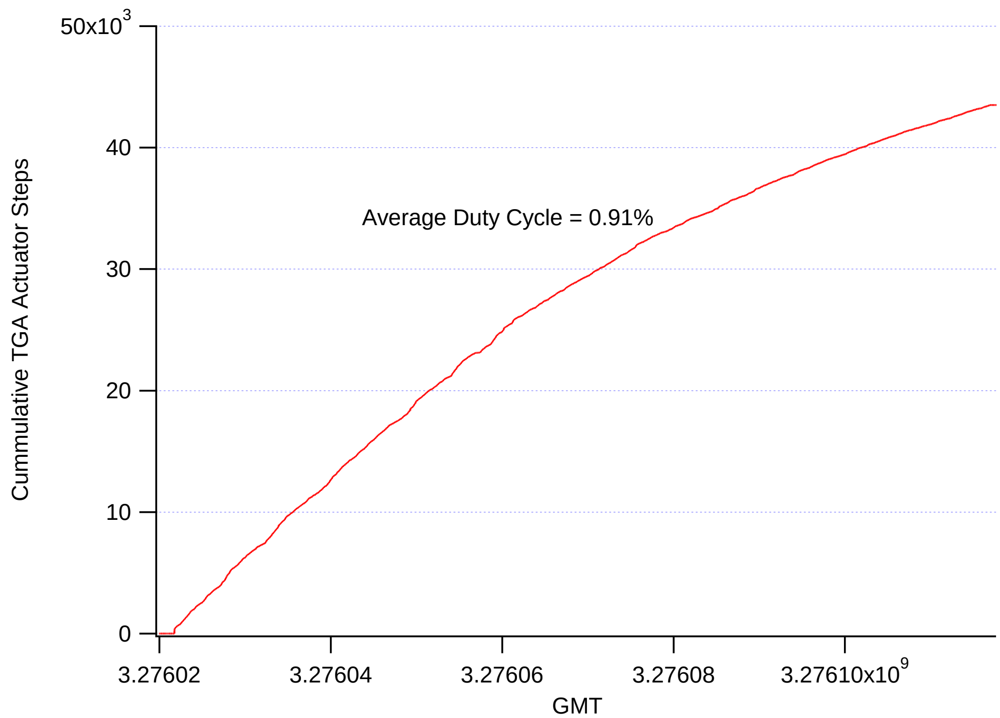

Fig. 6. TGA actuator step in thrust vector control mode during the 28-hr long FT1 characterization test

The IPS is designed so that the entire Dawn mission can be accomplished with just two ion thrusters. With the completion of the checkout of FT1 on October 25, 2007, two ion thrusters (FT1 and FT3) were fully checked out within 30 days after launch.

FT2 Performance Characterization

The outboard thruster on the +X side of the spacecraft, FT2, was started on DOY 2007-318, 52 days after launch. After the 6-minute cathode pre-heat both cathodes lit immediately upon application of the start voltages and the thruster was successfully started at ML27. Performance characterization for FT1 followed the same procedure used for FT3 and FT2 starting with 11 hours of operation at ML27 and stepping up in power to ML28 and then ML69, but with only three hours at each of these throttle levels. Operation at higher power levels was not attempted with FT2 at this time. The sun angle on the spacecraft at the time of this test resulted in higher than expected temperatures for the FT2 gimbal pads. While these higher temperatures were not a threat to the health of the thruster, they were sufficiently high that operation at ML90 or ML111 may have resulted in exceeding the fault protection temperature limits assigned for the gimbal pads. Rather than change the fault protection limits for FT2 it was decided to simply eliminate operation at ML90 and delay operation at ML111 until a more favorable sun angle could be used. This was done the next day (on DOY 2007-319). In the performance characterization test series FT1 was operated continuously for 19 hrs including 12 hours at ML27 and 3.5 hours each at ML48 and ML69. The following day FT2 was operated for four hours at ML111 and for another four hours at ML111 on DOY 2007-320.

The key electrical parameters for FT2 over the 18-hr performance characterization test are given in Fig. 7. There was only one high voltage recycle in the 14 first hours after the application of high voltage and 21 over the 18-hr test.

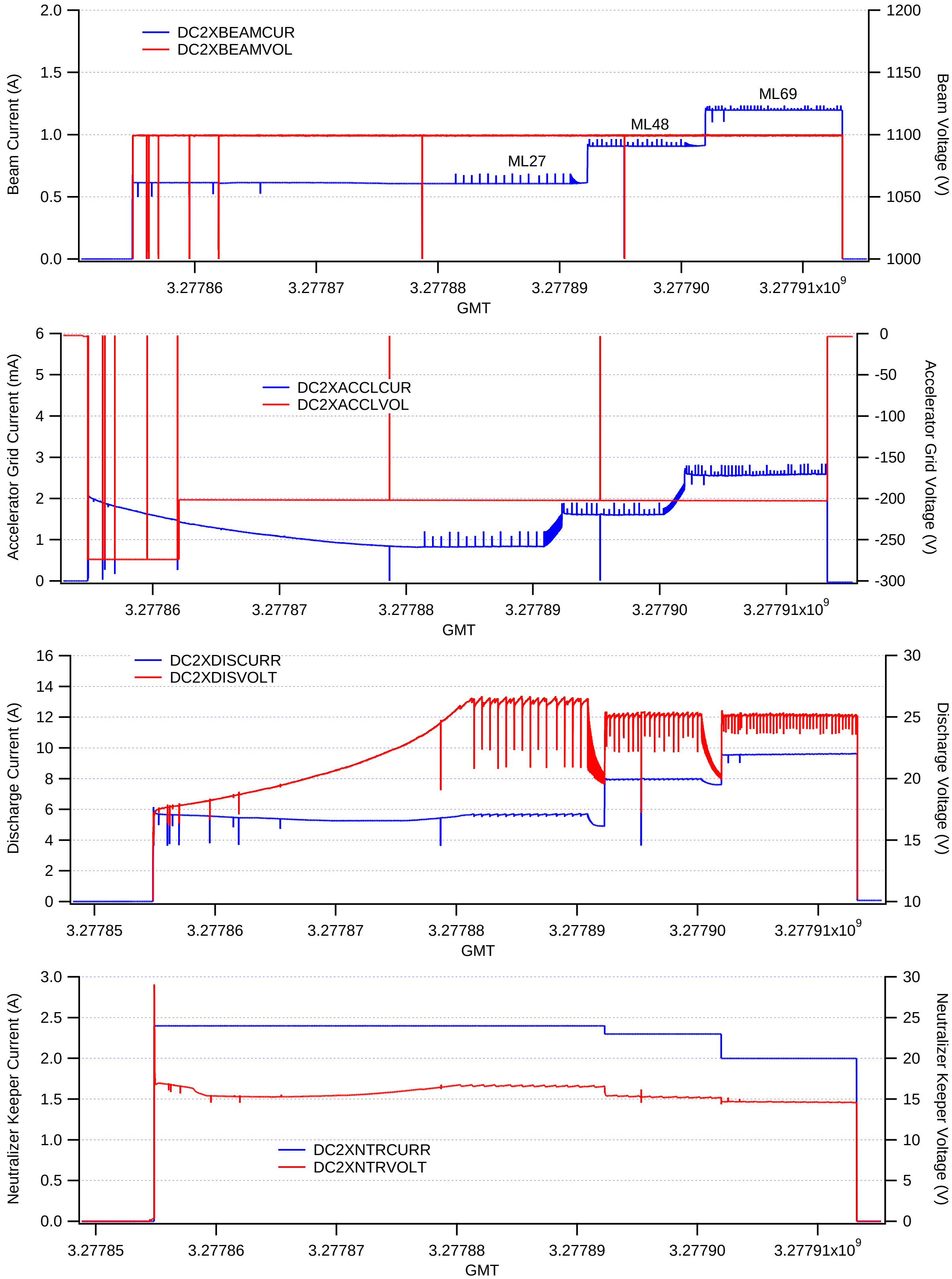

Fig. 7. Electrical parameters from the 18-hr long FT2 characterization test.

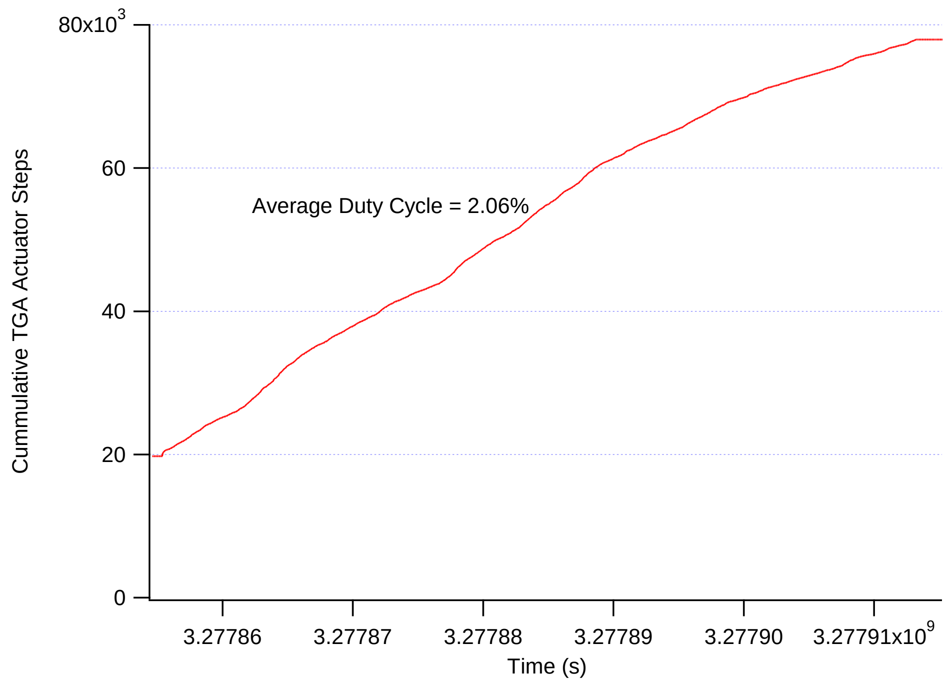

Fig. 8. TGA actuator step in thrust vector control mode during the 18-hr long FT2 characterization test.

The thruster electrical performance from the in-flight characterization test is compared to that from the ground thruster acceptance test in Table 6. These data indicate that the thruster and PPU operation in-flight is very similar to that observed on the ground. Thrust vector control of the spacecraft with FT1 was initiated within three minutes after the thruster was first started at ML27. The TGA actuator duty cycle over the 18-hr characterization test of FT1 was 2.1%. The cumulative number of steps over the 28-hr test period is given in Fig. 8. This value is higher than for FT1 or FT3 because the characterization test of FT2 was limited to the lower power and thrust levels, which result in higher actuator duty cycles.

Comparison of Measured and Predicted Thrust

The thrust was measured for each thruster, using the technique described in Ref. [13], at each of the five throttle levels: ML27, ML48, ML69, ML90, and ML111 (with the exception of FT2 in which the thrust was not measured at ML90). At each throttle level the thruster was operated long enough to reach a steady-state temperature (with the only exception being FT3 at ML111). However, the thrust measurements showed essentially no difference in thrust prior to reaching the steady-state temperature.

The measured thrusts (called "Actual") are compared to the pre-flight expected values for each thruster in Table 7. These data indicate excellent agreement with the pre-flight predictions and very little thruster-to-thruster differences.

The pre-flight expected values for the thrust were calculated using the standard equation for thrust from an ion thruster:

$$T = \alpha F_T J_B \sqrt{\frac{2 m_i V_N}{e}} \ , \tag{1}$$

where α is the thrust loss due to double ions, F_T is the thrust loss to due beam divergence, J_B is the beam current, m_i is the mass of a xenon ion, V_N is the net accelerating voltage, and e the electron charge. The beam current is the current measured by the beam supply, J_S, minus the current measured by the accelerator grid power supply, J_A, i.e., $J_B = J_S - J_A$. The pre-flight "expected" values for J_A are given in

Tables 4-6. The net accelerating voltage is the measured beam supply voltage, V_B, minus the neutralizer coupling voltage V_{NC}, i.e., $V_N = V_B - V_{NC}$. The neutralizer coupling voltage is not measured on the Dawn spacecraft and was assumed to be 14V ± 5V in the thrust calculations.

Double Ion Thrust Loss: The double ion thrust loss factor is calculated from the ratio of double-to-single ion beam currents,

$$\alpha = \frac{1 + \frac{\sqrt{2}}{2} \frac{J_B^{++}}{J_B^{+}}}{1 + \frac{J_B^{++}}{J_B^{+}}} \quad . \tag{2}$$

The double-to-single ion beam current ratio was measured in two different ways on two physically different, but functionally equivalent thrusters. During the extended life test (ELT) of the DS1 flight spare thruster, the double-to-singe ion beam current ratio was measured periodically throughout the test [12]. The ExB probe used to make these measurements provided double-to-single ion current ratios that corresponded to the average values across a “slice” of the ion beam spanning the full discharge chamber diameter as indicated in Fig. 9. These measurements were made at selected throttle levels spanning the full throttle range of the thruster. The second set of double-to-singe ion current measurements were made on the thruster designated EMT4 fabricated by NASA GRC during the NSTAR project. This thruster is functionally equivalent to the DS1 flight spare thruster fabricated by Hughes Electron Dynamics Devices (now L-3 Communications Electron Technologies, Inc). The measurements on EMT4 used an ExB probe that viewed a 1-cm diameter spot on the physical centerline of the thruster. These measurements were made at the same throttle levels over the thruster’s full throttle range as in the ELT. The results of these measurements are given in Table 8. The uncertainties given in this table are the 1-σ variations observed during the ELT.

The double ion thrust loss factor in Eq. (2) requires the ratio of the total double to single ion currents emitted by the thruster. Neither of the measurements described above provide this information. Therefore, these data were used to estimate the total ratio of double-to-single ion current in the beam. This was done by assuming that the ratio of double-to-single ion current measured on the thruster centerline was constant out to some critical radius, r_c, and zero from that radius to the edge of the grid. Using measurements of the total ion beam current density as a function of radial position across the grid, the value of r_c was selected so that the calculated double-to-single ion current ratio across the thruster diameter was equal to the measured slice value for each throttle level. This process separates the double ion current density from the single ion current density as a function of grid radius. The total double-to-single ion current ratio is then simply determined by integrating these two current density profiles over the grid area and taking the ratio. The end result of this process is given in Table 8 and Fig. 10.

Beam Divergence Thrust Loss: The ion beam divergence was measured multiple times over the full throttle range during each thruster acceptance test. The thrust loss based on the beam divergence data from the Dawn FT1 acceptance test is given in Fig. 11. A sufficient number of measurements were made at each throttle level to calculate the 1-σ variations, which are also shown in this figure.

The double-ion and beam-divergence thrust losses from Figs. 11 and 12 were used in Eq. (1) to calculate the expected thrust values in Table 7.

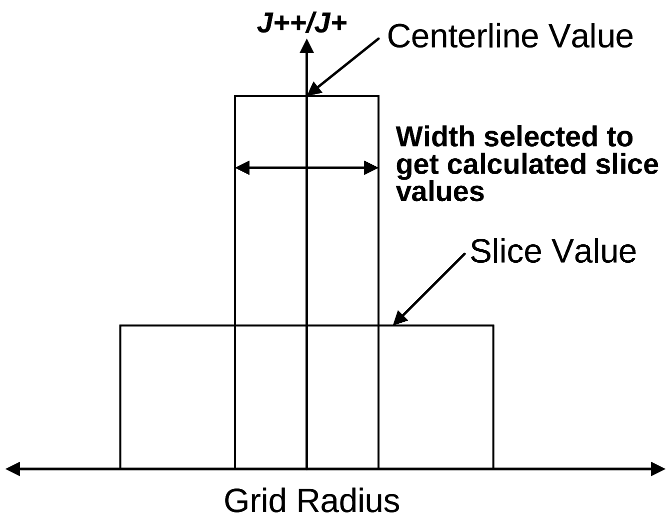

Fig. 9. Determination of the double-to-single ion current ratio.

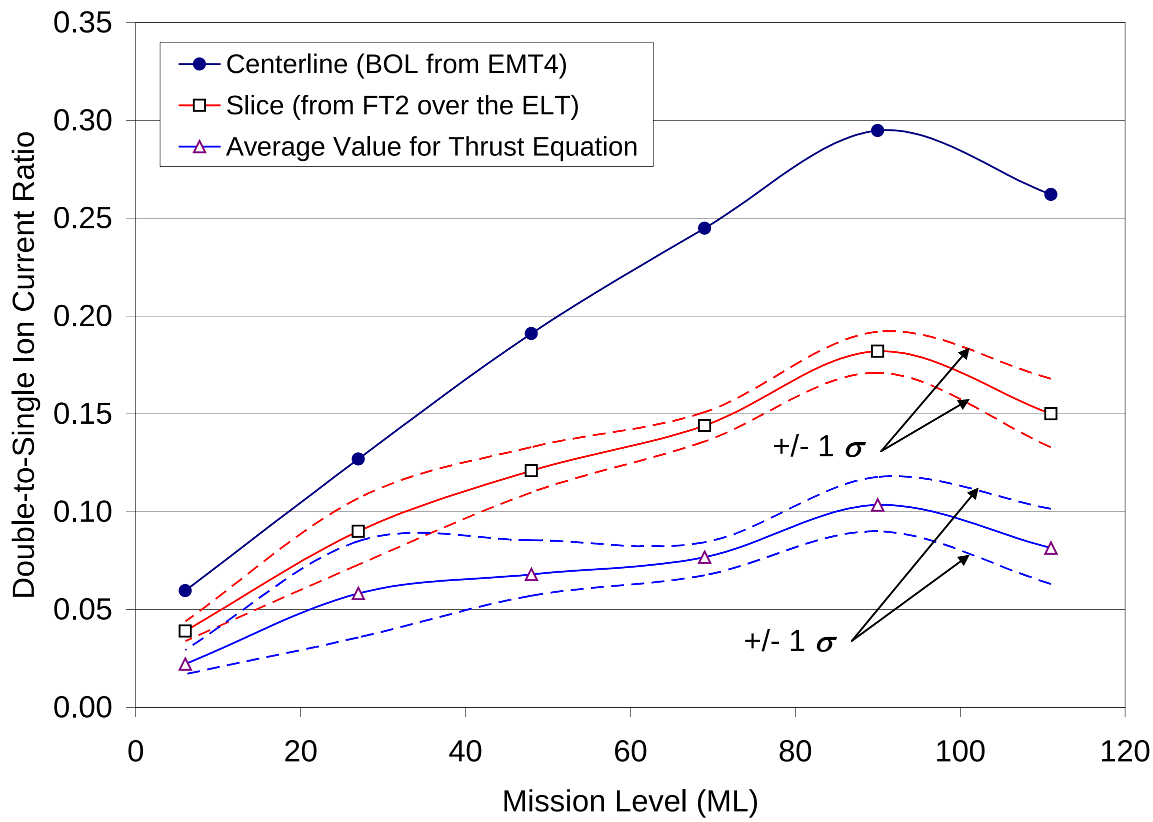

Fig. 10. Double-to-single ion currents vs mission level.

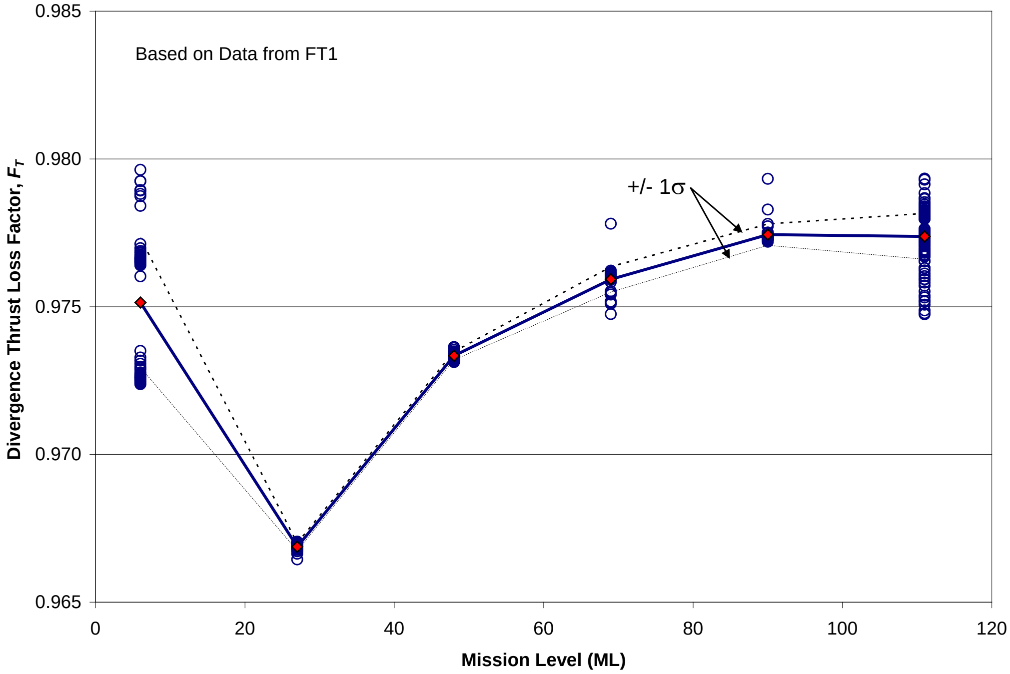

Fig. 11. Measured beam divergence thrust loss factor from the acceptance test of FT1. The red data symbols indicate the average values at each mission level.

Measured Roll Torque

It was observed on DS1 that the NSTAR ion thruster produces a roll torque about the thrust axis. For DS1 this torque was estimated to be about 10 μNm when the thruster was operated at the low-power end of the throttle range (ML10 to ML20). On Dawn measurements of the roll-torques produced during thruster operation were obtained from the momentum buildup in the Reaction Wheel Assemblies (RWAs) while in thrust-vector control mode. The results of these measurements are given in Fig. 12 for all three thrusters. These data indicate that FT2 is the best thruster, i.e., has the lowest roll torque magnitude, and produces a torque in the opposite direction from the other two thrusters. This is interesting since FT2 has a magnetic field polarity that is reversed relative to the other two thrusters. It also has the most peaked beam profile, while FT3, which produces the largest roll torque, has the flattest beam profile. The direction of the roll-torque produced by FT2 corresponds to the right-hand-rule with your thumb pointing in the direction of the ion beam propagation.

Three mechanisms for the production of this roll torque were evaluated during the Dawn IPS development: magnetic field effects; grid clocking errors; and neutralizer misalignment. The magnetic field induced roll torque considers the bending of the accelerated ion trajectories by the magnetic field from the discharge chamber that "leaks" through the grids. This mechanism produces roll torques that are in the observed directions for all three thrusters and produces the correct relative magnitudes for the thrusters. However, the absolute magnitudes are about a factor of ten less than that observed. Angular misalignment of the neutralizer is also completely inadequate to produce the observed roll torques for any reasonable misalignments. Grid clocking errors, where the accelerator grid has a systematic rotation about the grid centerline relative to the screen grid, can in principle produce the observed roll torques for relatively small errors. For example, a systematic clocking error that produces a screen grid to accelerator grid aperture misalignment of 25 μm (0.001") at the outer most radii of holes is sufficient to produce a roll torque of 60 μNm at ML111 for the ion beam profile typical of the NSTAR thruster.

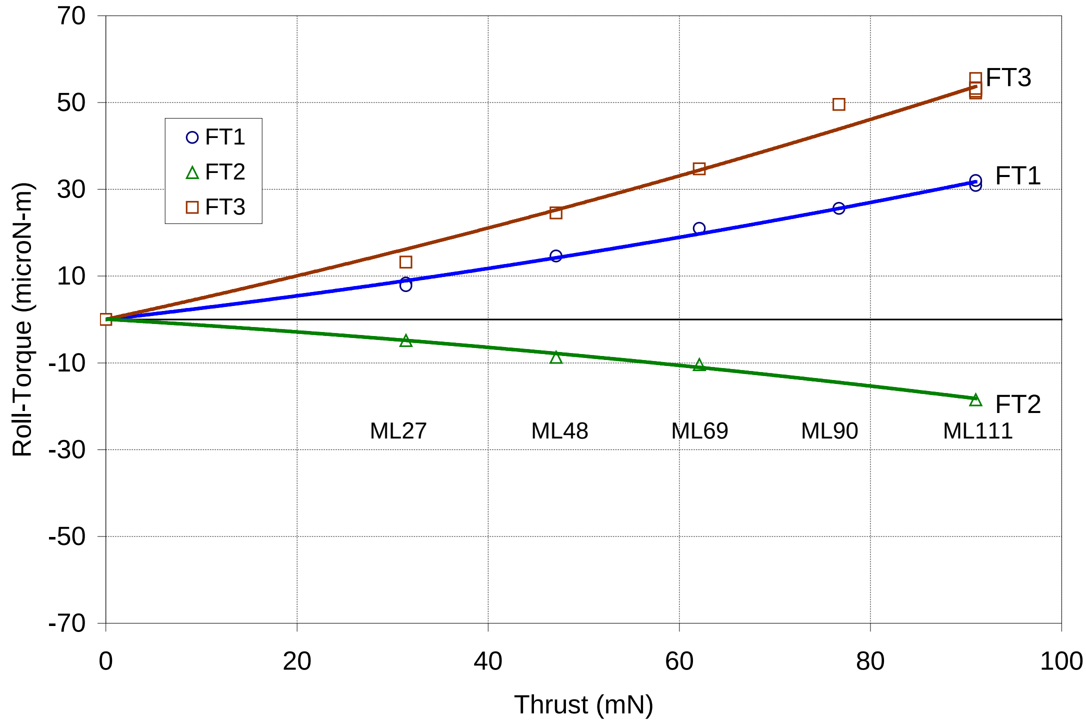

Fig. 12. Measured roll-torques produced by the Dawn ion thrusters.

IV. Long-Duration System Test (LDST)

A long-duration system test was performed in which the test was designed to mimic the procedure that was going to be followed during the first four years of normal thrusting-cruise operations for the heliocentric transfer to Vesta. During thrusting-cruise the plan is to operate the IPS at full power for approximately a week, then shut down, rotate the spacecraft to point the high-gain antenna at Earth and down link the data from that week of thrusting. After completion of the data transmission, the thruster is restarted in diode-mode to preheat it while the spacecraft is rotated back to the thrust attitude. Once in the thrust attitude the thruster is restarted at full power for another week of thrusting.

The LDST mimicked this process by operating FT3 for 167 hours, then terminating thrust for 4 hours, restarting FT3 in diode-mode for 1 hour, and then starting FT3 at ML111 and operating there for an additional 4 hours. These last four hours were to simulate start of the following week's thrusting. The results from the LDST are given in Figs. 13-20. The thruster's electrical parameters in Fig. 13 indicate very stable thruster operation over this test. There was a slight increase in the accelerator grid current which reached a steady-state value of approximately 6 mA. This is believed to be correlated to the slight decrease in the discharge voltage over this time. The neutralizer common voltage (measured as the voltage between neutralizer common and the spacecraft ground) is given in Fig. 14. These data indicate a neutralizer common voltage of approximately 2V. Also shown in this figure is the output from the neutralizer plume-mode detection circuit. The value of ~1.1V shown is indicative of operation in the proper mode. The unregulated 100-V bus input to the PPU is given in Fig. 15 during the LDST. The step-function change in array voltage at the left-hand-side of this figure is the result of the thruster start and the corresponding power draw. The slow increase in bus voltage is the result of the increase in solar range over the week-long LDST. The solar array current shows a corresponding slow decrease as the PPU regulates the current drawn to maintain operation of the thruster at constant power. The step-function increase in array voltage at the end of the test is the result of the thruster being shutdown. There were very few high voltage recycles over the LDST as indicated in Fig. 16. After a higher initial rate, the steady-state high-voltage recycle rate reached an average of approximately 1.5 recycles/day at ML111.

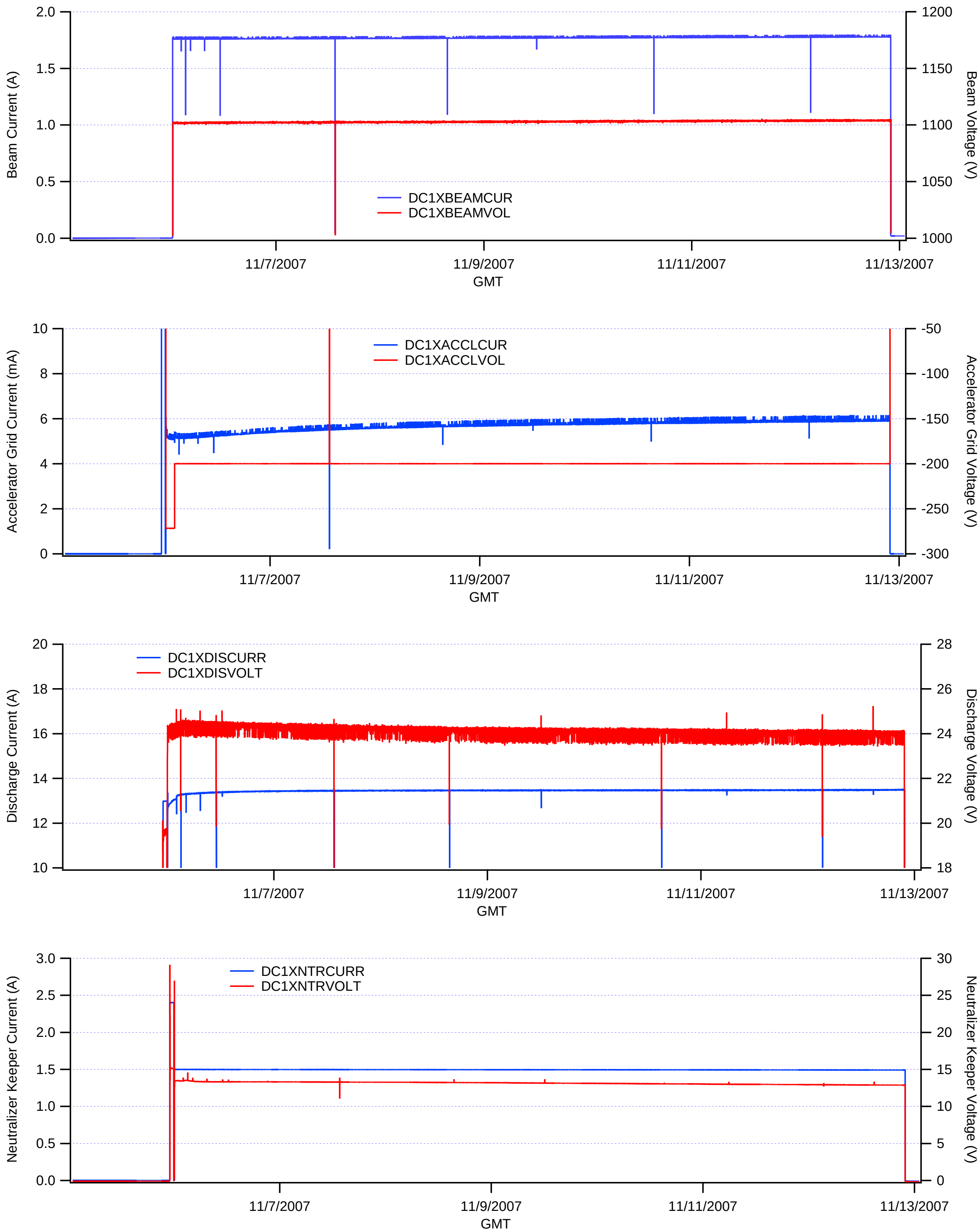

Fig. 13. Electrical parameters from FT3 during the long-duration system test (LDST).

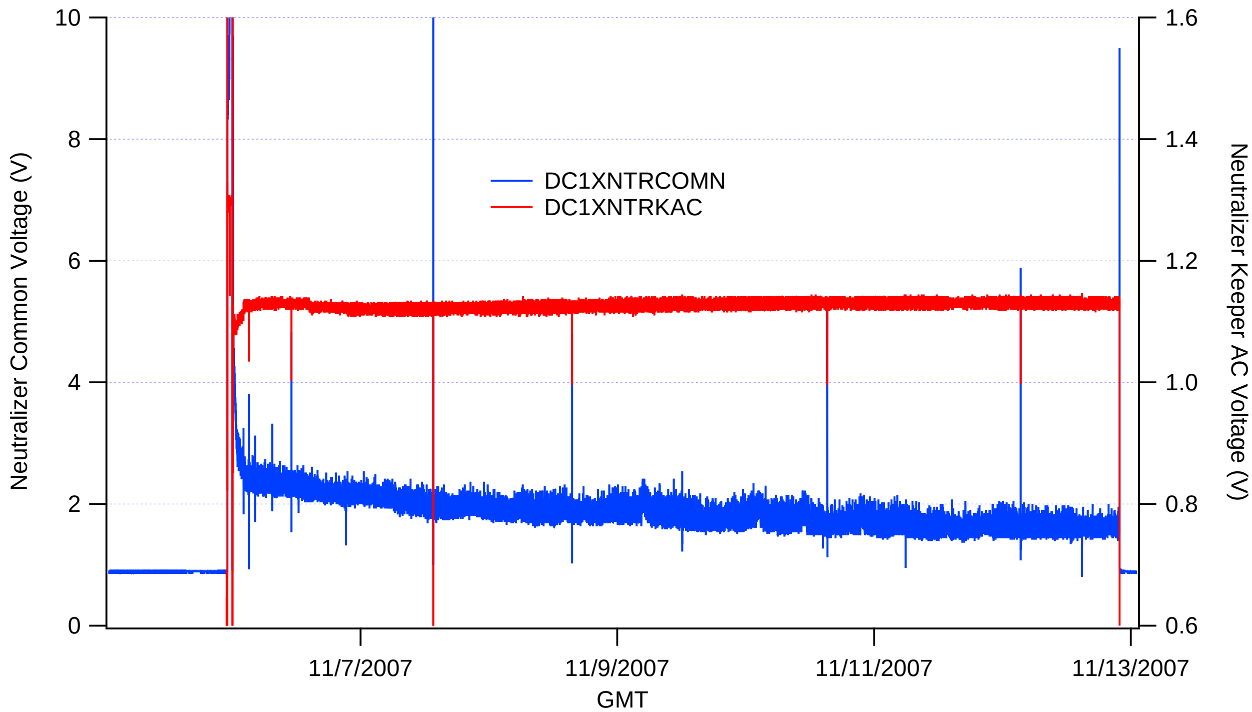

Fig. 14. Neutralizer common and the neutralizer keeper plume-mode circuit voltage over the LDST.

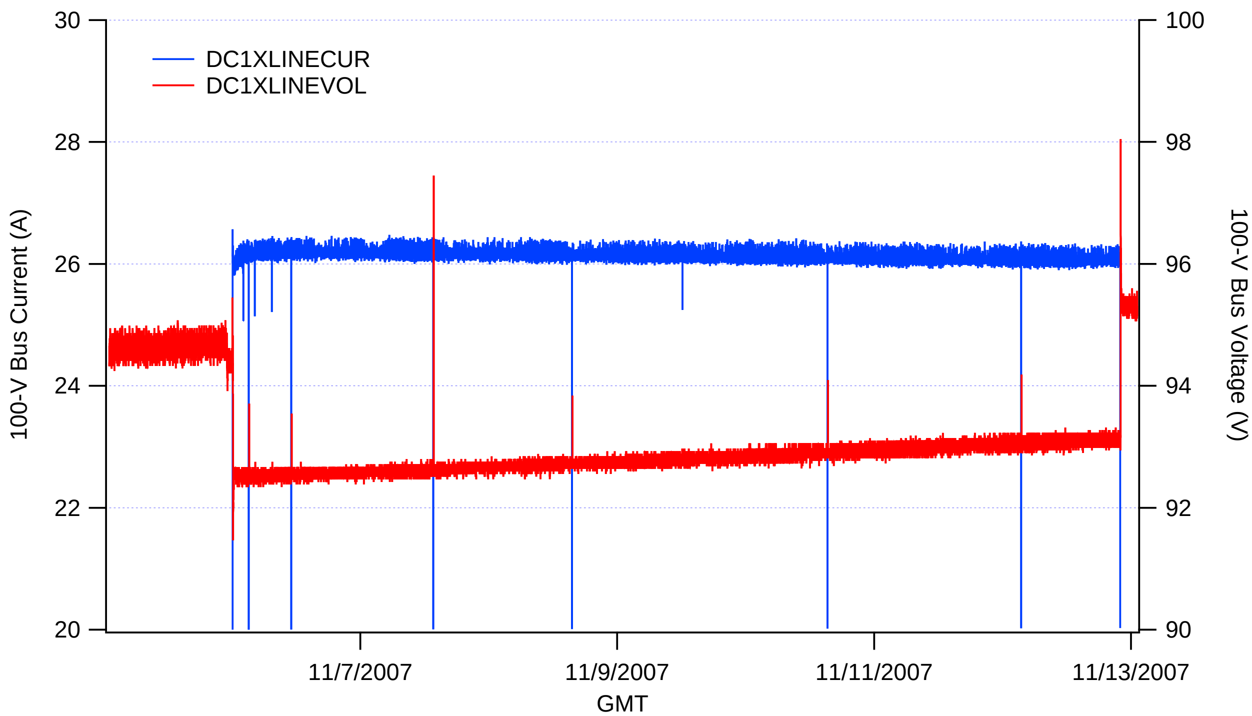

Fig. 15. 100-V bus voltage over the LDST. The observed increase in the bus voltage is due to the increase in solar range during the week-long test.

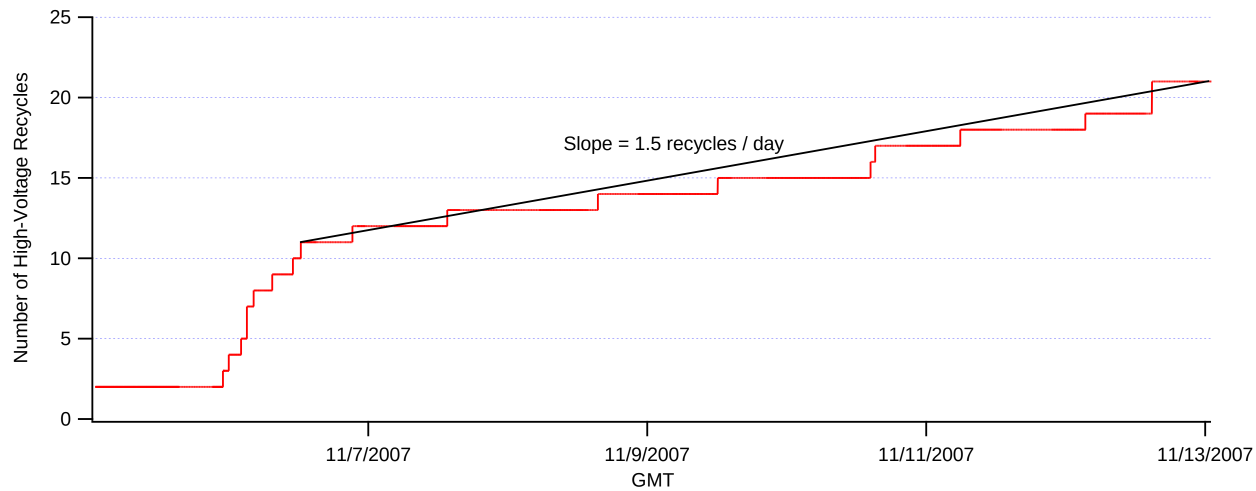

Fig. 16. High-voltage recycle rate during the long-duration system test averaged 1.5 recycles / day after the start-up initial transient.

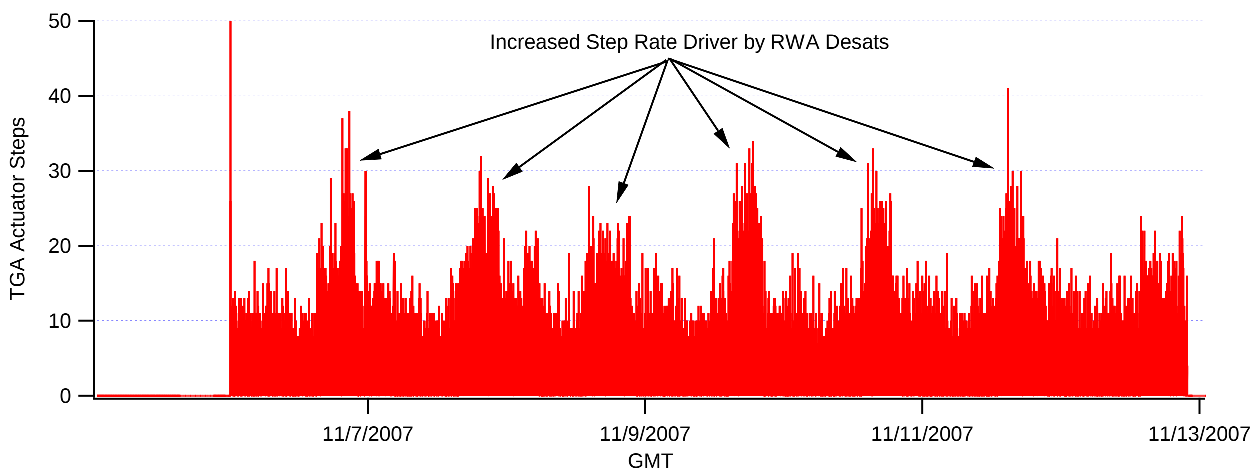

Fig. 17. Number of TGA actuator steps per 10-second interval over the LDST.

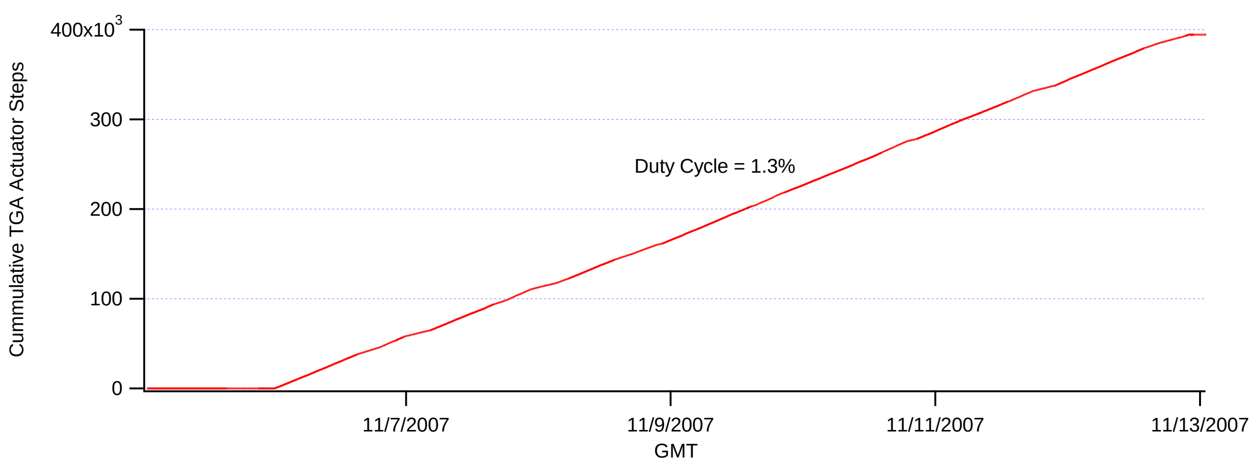

Fig. 18. TGA actuator step rate driven by RWA desats during the long-duration system test resulting in an actuator duty cycle greater than 1%.

The number of TGA actuator steps (per 10-second interval) are given in Fig. 17 for one of the two actuators in the FT3 TGA over the LDST. The peaks evident in this figure correspond to the planned desaturation events for the RWAs. The RWA desaturations (desats) are performed by the hydrazine thrusters in the reaction control system which dump the momentum built up due to the roll-torque produced by the ion thruster. This produces a disturbance in the spacecraft attitude which then produces an increase in the TGA step rate. The corresponding duty cycle for the TGA actuator over the LDST is given in Fig. 18. These data indicate an average duty cycle of 1.3% during the LDST. While this is higher than the 1% expected, it will not be an issue for the actuator life.

The internal PPU temperatures are given in Fig. 19. These temperatures are measured at four locations inside the PPU: the baseplate; the discharge power supply, the beam supply, and the neutralizer supply. The baseplate temperature indicated by the blue line is only about 27C with the PPU operating at full power.

The steady-state gimbal actuator temperatures, as indicated in the bottom chart in Fig. 20, are only 29C. The thruster temperatures during the LDST are shown in the top chart in Fig. 20. The temperatures at the thruster gimbal mounting pads are indicated to be between 118C and 126C, and the temperatures on the thruster's front mask are only 88C.

The main solenoid valve cycle rate measured during the LDST averaged 19.2 cycles/hr. This is about 1.7 times the expected cycle rate of 11.1 cycles/hr. Similarly, the cathode solenoid cycle rate was 5.6 cycles/hr when the expected rate was 3.4 cycles/hr. Subsequent analyses indicated that the expected values did not properly account for the temperature difference between the xenon tank and the solenoid valves. During thrusting, the xenon tank temperature was at least 3C less than the solenoid valve temperature. During operation of the bang-bang pressure regulation system the upstream solenoid valve is held open long enough for the pressure in the volume between solenoid valves to equilibrate with the tank pressure. However, since the solenoid valve temperature is greater than the tank temperature, the density of xenon in the volume between the solenoid valves is less than that in the tank. Therefore, calculations based on the tank temperature will under predict the required solenoid valve cycle rate. Once the temperature difference was accounted for good agreement with the measured solenoid valve cycle rates was obtained.

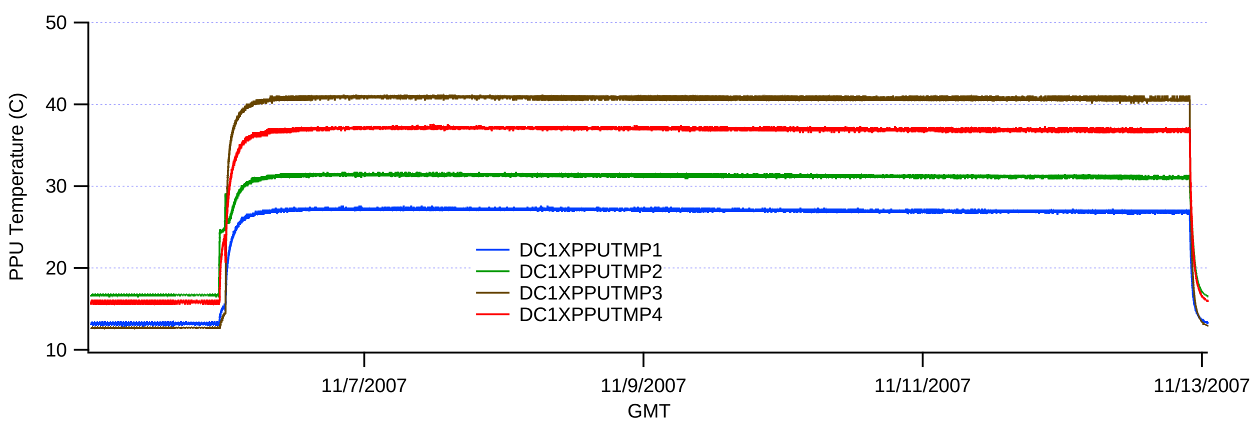

Fig. 19. Measured internal PPU temperatures during the LDST. The PPU temperatures 1 through 4 correspond to internal measurements of the baseplate, the neutralizer power supply, the beam power supply, and the discharge power supply, respectively.

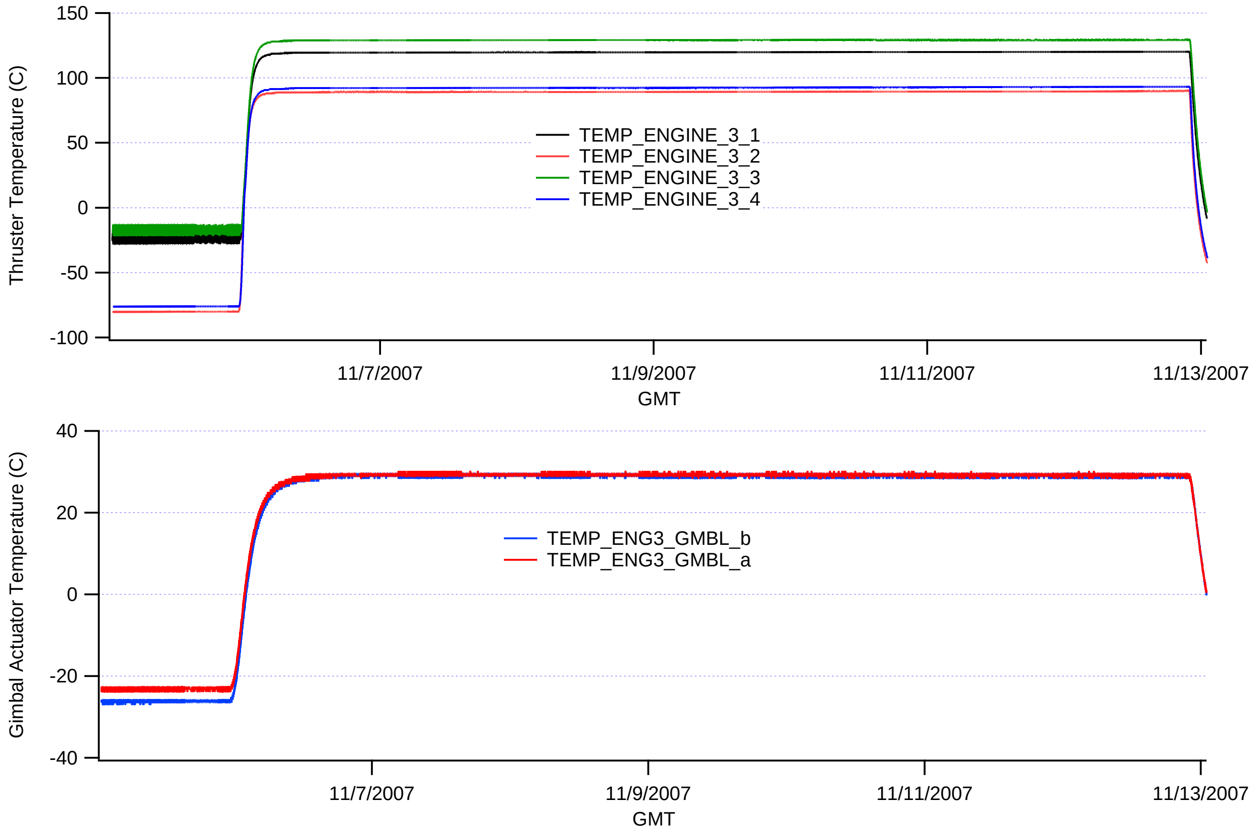

Fig. 20. Measured FTE and its gimbal actuator temperatures during the LDST. For the ion thruster TEMP_ENGINE_3_1 and TEMP_ENGINE_3_3 are temperatures of the thruster the gimbal pads and TEMP_ENGINE_3_2 andTEMP_ENGINE_3_4 correspond to temperatures measured on the front mask.

V. Other Interesting Phenomena

The ion propulsion performed almost exactly as expected during the initial checkout phase of the Dawn mission. Nevertheless, there were some interesting phenomena identified as discussed below.

Accelerator Grid Voltage Change

The first interesting phenomena is associated with the accelerator grid voltage. Each the thruster is started the accelerator grid voltage is maintained at -275V for the first two hours. This is done to assure that no electron-backstreaming occurs during the thermal transient as the thruster heats up to it normal operating temperature. This thermal transient causes a temporary decrease in the grid-to-grid gap in the ion accelerator system [14]. After two hours the accelerator grid voltage is changed to its normal operating voltage of -200V. Incredibly, the attitude control system (ACS) can sense this change in accelerator grid voltage because it creates a disturbance to the spacecraft attitude. This occurs because the change in accelerator grid voltage produces a small decrease in the thrust level. The decrease in thrust must be accounted for by the ACS which is using the ion thruster for pitch and yaw control of the spacecraft. The ACS is constantly making small adjustments to the thrust vector location. The step-function decrease in thrust means the thrust vector is no longer pointing in the correct direct and the ACS responds with larger-than-normal movements of the thruster gimbal until the disturbance is damped out.

Thrust Measurement Sensitivity

The second interesting phenomenon is that when making thrust measurements the radiometric technique [13] is sufficiently sensitive that it can detect a single high-voltage recycle event. Even more incredible, this technique can actually make good estimates of the duration of a recycle event (which typically lasts for about 1.5 seconds).

Xenon Tank Temperature

The third interesting feature is associated with the temperature measurements on the xenon tank. There are four temperature sensors located at physically different locations on the exterior of the xenon tank. When the IPS is not thrusting, sensors 1 and 2 typically indicate temperatures that are approximately 1C to 2C greater than sensors 3 and 4, but during thrusting this temperature difference disappears as indicated in Fig. 21. This occurs even if no xenon is being drawn from the tank, which was the situation at the start of each thruster characterization test in which each thruster was operated for several hours entirely from the xenon in the plenum tanks. When thrusting stops, the temperature difference is re-established. This phenomenon is very repeatable and occurs every time the IPS is operated. The saw-toothed pattern in the temperatures indicated by sensors 3 and 4 in Fig. 21 result from heater cycling. The period between temperature peaks is approximately 0.5 hours.

Another interesting feature is also associated with the xenon tank temperature measurements. In Fig. 21 it was indicated that the temperature peaks about every 30 minutes due to heater cycling. However, during IPS thrusting not only do the temperature differences between the various temperature sensors decrease, but the period between temperature peaks starts to increase. During the LDST the IPS was operated long enough for a new steady-state period between temperature peaks to be established. This new period was 11.2 hours, more than 22 times longer than the period between peaks when the IPS is not thrusting. The xenon tank temperature data from the LDST is given in Fig. 22 and shows the 11.2-hr period between temperature peaks. These peaks are not an issue for the flight system, but the cause for the change in the heater cycle period from 0.5 hours when not thrusting to 11.2 hours when thruster is currently unknown.

Neutralizer Common Voltage

During an attempt to run ion thruster FT2 at ML111 for a characterization test on DOY 2008-099, an unexpected shutdown occurred during the diode-mode preheat of the thruster. Telemetry indicated a Neutralizer Common Error was detected by the DCIU flight software (FSW) causing the DCIU to terminate diode-mode operation. A Neutralizer Common Error occurs when the neutralizer common voltage – the voltage between spacecraft ground and the neutralizer cathode – exceeds a preset limit of +40 V.

As described by Goebel and Katz [15], large positive values of the neutralizer common voltage can be caused by an interaction of the plasma created by the thruster and the high-voltage solar array. During thruster operation either in diode-mode or normal thrusting, this plasma interacts with the high-voltage solar arrays to drive the spacecraft ground potential negative of the ambient space plasma potential. The plasma created by the thruster is denser in diode-mode because of the lower ion velocities aggravating this effect. This denser plasma can result in the spacecraft ground potential being driven several 10’s of volts negative of the space plasma potential. The thruster’s neutralizer, however, clamps neutralizer common to within 15V of the space plasma potential. In the Dawn PPUs the impedance between neutralizer common and the spacecraft ground is 1.4 megaohms which is sufficiently large that a voltage difference of 10’s of volts can be established between neutralizer common and the spacecraft ground.

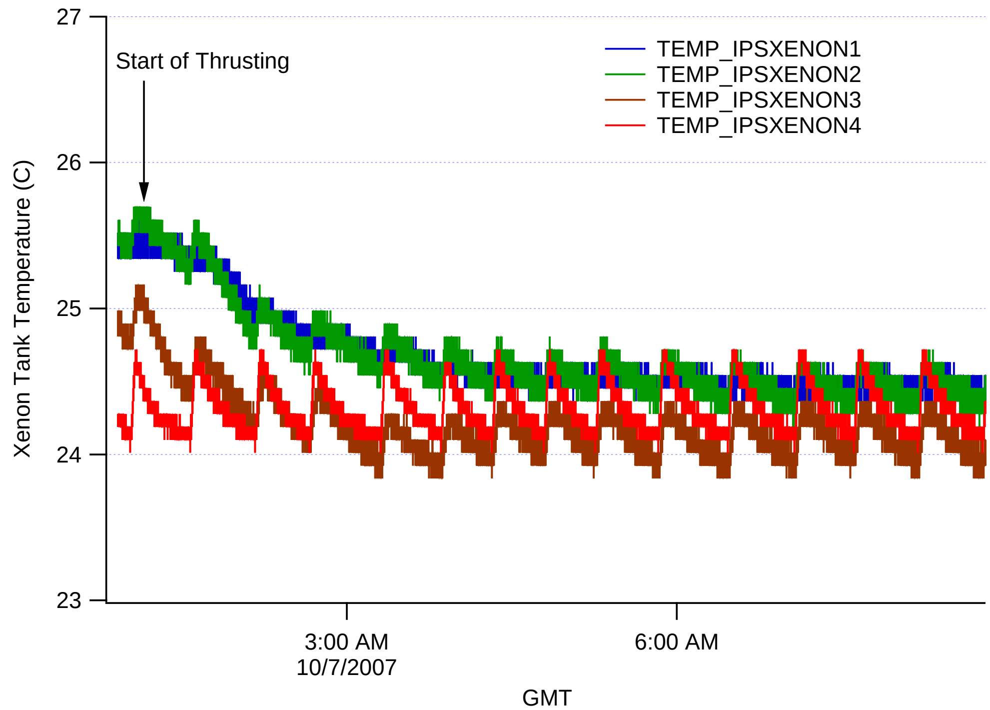

Fig. 21. Xenon tank temperature measurements during the first part of the FT3 characterization test at ML27. No xenon flow from the Xe tank occurred during the time frame shown in this figure (all the xenon flow to run the thruster came from the plenum tanks). The time between temperature peaks for sensor 4 is approximately 0.5 hrs.

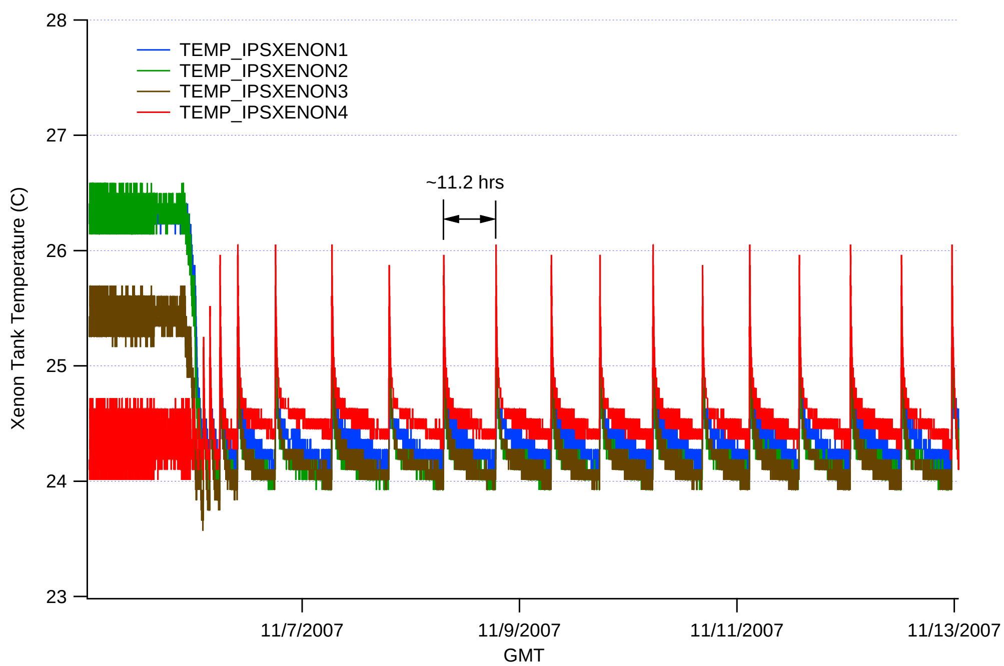

Fig. 22. Xenon tank temperature measurements during the LDST showing the 11.2-hr period between temperature peaks.

Under these conditions, and as first observed by Brinza [16] the neutralizer common voltage is a function of the spacecraft attitude (and therefore, a function of the thruster being used on Dawn) and the solar array voltage. The solar array output voltage increases with solar range and the maximum neutralizer common voltage measured during the diode-mode preheat follows this increase as indicated in Fig. 23. In this figure, increasing calendar time corresponds to increasing solar range causing both the solar array voltage and the maximum neutralizer common voltage to increase. Since this is a normal, and well understood, behavior of the flight system, subsequent shutdowns due to Neutralizer Common Errors were prevented by changing a parameter in the data tables stored in each DCIU. This change effectively prevents the FSW from checking for Neutralizer Common Errors.

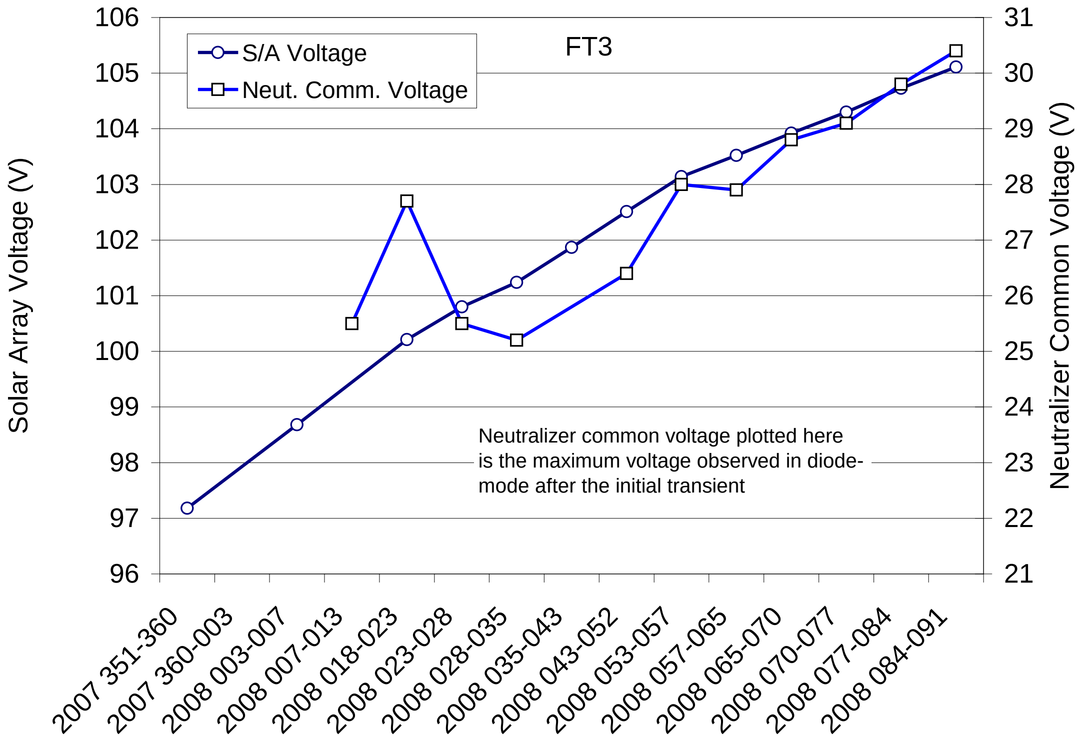

Fig. 23. Maximum observed neutralizer common voltage during diode-mode preheat increases with the solar array voltage.

VI. Conclusions

Checkout of the ion propulsion system was a principle component of the initial checkout activity of the Dawn spacecraft. This activity took place over the first 80 days after launch on September 27, 2007. The full Dawn mission can be accomplished with just two of three ion thrusters in the IPS. Within 30 days after launch checkout of two ion thrusters was complete. Checkout of all three thrusters was completed by November 30, 2007, 64 days after launch, and after operating the IPS for 285 hours and processing 3 kg of xenon.

Measurement of the thrust at five throttle levels covering the input power range from 900W to 2500W indicated that the thrust agrees well with the pre-flight expected values and that there is very little thruster-to-thruster difference. Electrical operating parameters for all three thrusters also agree well the preflight expected values based acceptance testing performed more that two years earlier. These data confirmed that there are three healthy thrusters on the spacecraft. Operation of both PPUs in the IPS was demonstrated over the same power range (900W to 2500W). PPU efficiency measurements agree well with pre-flight values over the full throttle range. Internal temperature measurements indicate that the spacecraft's thermal control system does an outstanding job of rejecting the PPU's waste heat at full power as expected.

All three thruster-gimbal assemblies were found to still be in their launch position after launch as expected, and all three were demonstrated to be fully functional. Operation of each thruster in thrust vector control mode was successfully demonstrated. The gimbal actuator duty cycle during long-duration operation in thrust vector control mode was found to be 1.3%. This was a little higher than the expected 1%, but is well within the life capability of the actuators, which were tested to 18 times the required life assuming a 1% duty cycle.

All components of the xenon feed system were in good health after launch and are functioning as expected. The pressures in the xenon tank and in the two plenum tanks after were launch were as expected indicating that none of the closed latch valves changed states or leaked during launch. In addition, subsequent operation of all thee ion thrusters indicated that none of the latch valves that were launched open changed state during launch. The xenon feed system operated exactly as expected throughout the checkout activities with the exception that the solenoid valve cycle rate was higher than predicted. Subsequent analyses that correctly accounted for the temperature difference between the xenon tank and the solenoid valves agreed well with the measured rates.

At the end of the Dawn spacecraft checkout period the ion propulsion system had successfully completed all planned test activities and was ready for the start of deterministic thrusting.

Acknowledgments

The Dawn IPS is the result of combined work of very many talented people at JPL, Orbital Sciences, Corp., GRC, and at the vendors supplying major IPS components: Moog for the XCA, Carleton Technologies for the Xe tank, L3 Communications Electron Technologies, Inc. for the thrusters and PPUs, and Starsys for the TGA gearmotors. The authors gratefully acknowledge the contributions of these organizations and the people in them. This research was carried out, in part, at the Jet Propulsion Laboratory, California Institute of Technology, under a contract with the National Aeronautics and Space Administration.

References

1. Rayman, M. D., Fraschetti, T. C., Raymond, C. A., Russell, C. T., Dawn: A Mission in Development for Exploration of Main Belt Asteroids Vesta and Ceres," Acta Astronautica 58 (2006 605-616).
2. Russell, C.T., et al., "Dawn: A Journey in Space and Time," Planetary and Space Science 52 (2004) 465-489.
3. Brophy, J.R., Rayman, M.D., Pavri, B., "Dawn: An Ion-Propelled Journey to the Beginning of the Solar System," IEEEAC paper #1504, presented at the 2008 IEEE Aerospace Conference, March 1-8, 2009, Big Sky, Montana.
4. Brophy, J.R., et al., "The Dawn Ion Propulsion System – Getting to Launch," IEPC-2007-083, Presented at the 30th International Electric Propulsion Conference, Florence, Italy September 17-20, 2007.
5. Brophy, J. R., et al., "Ion Propulsion System (NSTAR) DS1 Technology Validation Report," JPL Publication 00-10, October 2000.
6. Rayman, M. D., "The Successful Conclusion of the Deep Space 1 Mission: Important Results Without a Flashy Title," Space Technology 23, Nos. 2-3, p. 185-196 (2003).
7. Rayman, M. D. and Varghese, P., "The Deep Space 1 Extended Mission," Acta Astronautica 48, No. 5-12, pp. 693-705 (2001).

8. Polk, J.E., et al., ” Performance of the NSTAR Ion Propulsion System on the Deep Space One Mission, AIAA- 2001-0965, presented at the 39th AIAA Aerospace Sciences Meeting & Exhibit, 8-11 January 2001 / Reno, NV.
9. Brophy, J. R., et al., “Status of the Dawn Ion Propulsion System,” AIAA-2004-3433, presented at the 40th AIAA/ASME/SAE/ASEE Joint Propulsion Conference & Exhibit, 11-14 July, 2004, Fort Lauderdale, Florida.
10. Garner, C.E., et al., “In-Flight Operation of the Dawn Ion Propulsion System- The First Nine Months,” AIAA-2008-4916, presented at the 44th AIAA/ASME/SAE/ASEE Joint Propulsion Conference , 20-23 July, 2008, Harford, CT
11. Polk, J.E., et al., ” An Overview of the Results from an 8200 Hour Wear Test of the NSTAR Ion Thruster, AIAA 99-2446, presented at the 35th AIAA/ASME/SAE/ASEE Joint Propulsion Conference and Exhibit, 20-24 June 1999, Los Angeles, California.
12. Sengupta, A., et al., “An Overview of the Results from the 30,000 Hr Life Test of Deep Space 1 Flight Spare Ion Engine, AIAA-2004-3608, presented at the 40th AIAA/ASME/SAE/ASEE Joint Propulsion Conference and Exhibit, Fort Lauderdale, Florida, July 11-14, 2004.
13. McElrath, T. P., Han, D., and Ryne, M. S., “Radio Navigation of Deep Space 1 During Ion Propulsion Usage,” Paper MS00/57 presented at the 15th International Symposium of Spaceflight Dynamics, Biarritz, France, June 2000.
14. Diaz, E.M., and Soulas, G.C., “Grid Gap Measurement for an NSTAR Ion Thruster, NASA /TM—2006-214249, April 2006.
15. Goebel, D. and Katz, I., Fundamentals of Electric Propulsion: Ion and Hall Thrusters, JPL Space Science And Technology Series, March 2008, pp 415-418.
16. J.R. Brophy, D.E. Brinza, J.E. Polk, M.D. Henry, and A. Sengupta, “The DS1 Hyper-Extended Mission,” AIAA-2002-3673, July 2002.

Table 1. Summary of Key IPS Checkout Activities.

Event	Event Date	Mission Time	Power Level	Xenon Used	Event Duration	Cumulative Xe Used
	(DOY 2007)	(days after launch)		(g)	(hours)	(kg)
Launch	270	0	N/A	0.0	N/A	0.00
Propellant Line Bakeout	274	4	N/A	0.0	24.0	0.00
FT3 Cathode Conditioning	274	4	N/A	0.0	5.0	0.00
FT3 TGA Initialization	274	4	N/A	0.0	0.7	0.00
FT3 1st Diode Mode Bakeout	278	8	0	22.1	2.0	0.02
FT3 Main Plenum Blowdown	278	8	Blowdown	44.8	7.0	0.07
FT3 ICO ML27-ML111	280	10	27-111	165.8	25.2	0.23
FT3 Normal 1 Diode Mode	281	11	0	11.1	1.0	0.24
FT3 Normal 1	281	11	111	43.9	4.0	0.29
FT3 Normal 2 Diode Mode	282	12	0	11.1	1.0	0.30
FT3 Normal 2	282	12	111	39.0	3.5	0.34
FT3 Normal 2 Gyroless Diode	282	12	0	11.1	1.0	0.35
FT3 Normal 2 Gyroless	282	12	111	22.1	2.0	0.37
FT1 Cathode Conditioning	283	13	N/A	0.0	5.0	0.37
FT1 TGA Initialization	283	13	N/A	0.0	0.7	0.37
FT1 Diode Mode	283	13	0	23.0	2.0	0.39
FT1 Blowdown	283	13	Blowdown	46.3	7.0	0.44
FT1 ICO ML27	284	14	27	44.6	7.7	0.48
FT1 ICO Redo ML27-111	296	26	27-111	178.8	26.8	0.66
FT1 Normal 1 Diode Mode	298	28	0	10.7	0.9	0.67
FT1 Normal 1 Pointing Calibration	298	28	111	44.2	4.0	0.72
FT1 Normal 2 Diode Mode	298	28	0	10.6	0.9	0.73
FT1 Normal 2 Pointing Calibration	298	28	111	44.2	4.0	0.77
FT3 Gyrofull Desat Diode Mode	303	33	0	12.2	1.1	0.79
FT3 Gyrofull Desat ML111	303	33	111	32.9	3.0	0.82
FT3 Gyroless Desat Diode Mode	303	33	0	12.9	1.2	0.83
FT3 Gyroless Desat ML 111	303	33	111	32.9	3.0	0.86
FT2 Cathode Conditioning	305	35	N/A	0.0	5.0	0.86
FT2 TGA Initilization	305	35	N/A	0.0	0.7	0.86
FT2 Diode Mode Bakeout	305	35	0	4.8	0.4	0.87
FT3 LDST Diode Mode Bakeout	309	39	0	11.1	1.0	0.88
FT3 LDST ML111	310	40	111	1816.9	165.9	2.70
FT3 Normal 1 Diode Mode	317	47	0	11.0	1.0	2.71
FT3 Normal 1	317	47	111	43.8	4.0	2.75
FT2 ML27-69	318	48	111	139.9	16.3	2.89
FT2 Diode Mode-RWA	319	49	0	2.6	13.7	2.89
FT2 ML111-RWA	319	49	111	32.7	3.0	2.93
FT2 Diode Mode-Jets	320	50	0	10.5	1.0	2.94
FT2 ML111-Jets	320	50	111	33.0	3.0	2.97
FT3 FSW 7.0 Validation Diode Mode	334	64	0	10.9	1.0	2.98
FT3 FSW 7.0 Validation Ml111	334	64	111	43.7	4.0	3.02

Table3 Dawn IPS Throttle Table.

Mission Level (ML)	PPU Input Power (kW)	Thruster Input Power (kW)	Thrust (mN)	Total Flow (mg/s)	Isp (s)	Thruster Efficiency	Mission Level (ML)	PPU Input Power (kW)	Thruster Input Power (kW)	Thrust (mN)	Total Flow (mg/s)	Isp (s)	Thruster Efficiency
111	2483	2275	91.0	3.03	3060	0.601	55	1453	1332	51.7	1.75	3002	0.571
110	2465	2258	90.6	3.03	3046	0.600	54	1438	1317	51.3	1.75	2981	0.570
109	2447	2241	90.2	3.03	3032	0.599	53	1422	1303	50.9	1.75	2960	0.568
108	2429	2224	89.8	3.03	3017	0.597	52	1407	1288	50.6	1.75	2939	0.566
107	2411	2207	89.4	3.03	3003	0.596	51	1391	1273	50.2	1.75	2918	0.564
106	2393	2191	88.9	3.03	2989	0.595	50	1376	1259	49.8	1.75	2896	0.563
105	2375	2174	88.5	3.03	2974	0.594	49	1360	1244	49.5	1.75	2875	0.561
104	2354	2156	86.4	2.84	3098	0.609	48	1340	1226	47.1	1.60	3000	0.565
103	2335	2139	86.0	2.84	3083	0.608	47	1323	1210	46.7	1.60	2975	0.563
102	2316	2121	85.5	2.84	3067	0.607	46	1306	1194	46.3	1.60	2949	0.561
101	2297	2103	85.1	2.84	3051	0.605	45	1290	1178	45.9	1.60	2924	0.559
100	2278	2086	84.6	2.84	3035	0.604	44	1273	1162	45.5	1.60	2898	0.557
99	2259	2068	84.2	2.84	3019	0.603	43	1256	1146	45.1	1.60	2873	0.554
98	2240	2051	83.7	2.84	3003	0.601	42	1239	1130	44.7	1.60	2846	0.552
97	2229	2042	81.7	2.66	3128	0.614	41	1214	1106	41.8	1.45	2937	0.545
96	2211	2026	81.3	2.66	3112	0.613	40	1198	1091	41.5	1.45	2911	0.542
95	2193	2009	80.9	2.66	3096	0.612	39	1182	1076	41.1	1.45	2885	0.540
94	2175	1992	80.5	2.66	3080	0.610	38	1166	1061	40.7	1.45	2859	0.538
93	2157	1976	80.1	2.66	3064	0.609	37	1151	1046	40.3	1.45	2833	0.535
92	2139	1959	79.6	2.66	3048	0.608	36	1135	1031	40.0	1.45	2806	0.533
91	2121	1942	79.2	2.66	3032	0.606	35	1119	1016	39.6	1.45	2779	0.531
90	2105	1930	76.7	2.52	3099	0.604	34	1084	984	36.6	1.30	2864	0.522
89	2088	1914	76.3	2.52	3084	0.603	33	1068	968	36.2	1.30	2834	0.520
88	2071	1898	75.9	2.52	3068	0.602	32	1051	952	35.8	1.30	2803	0.517
87	2054	1883	75.5	2.52	3052	0.600	31	1034	936	35.4	1.30	2772	0.514
86	2037	1867	75.1	2.52	3036	0.599	30	1018	920	35.0	1.30	2740	0.511
85	2020	1851	74.7	2.52	3020	0.598	29	1001	904	34.6	1.30	2708	0.508
84	2003	1836	74.3	2.52	3004	0.597	28	984	888	34.2	1.30	2676	0.505
83	1982	1818	72.0	2.36	3113	0.605	27	952	858	31.4	1.16	2765	0.497
82	1963	1801	71.6	2.36	3095	0.603	26	928	835	30.9	1.16	2715	0.493
81	1944	1783	71.1	2.36	3076	0.602	25	904	811	30.3	1.16	2664	0.488
80	1925	1766	70.7	2.36	3057	0.600	24	879	788	29.7	1.16	2612	0.483
79	1906	1748	70.2	2.36	3038	0.599	23	855	765	29.1	1.16	2559	0.477
78	1887	1731	69.8	2.36	3019	0.597	22	831	742	28.5	1.16	2504	0.472
77	1869	1714	69.3	2.36	2999	0.595	21	806	719	27.8	1.16	2449	0.465
76	1847	1695	66.8	2.20	3101	0.600	20	788	701	26.2	1.09	2458	0.450
75	1826	1676	66.4	2.20	3079	0.598	19	774	689	25.9	1.09	2427	0.447
74	1806	1657	65.9	2.20	3057	0.596	18	761	676	25.5	1.09	2395	0.443
73	1786	1639	65.4	2.20	3036	0.595	17	748	664	25.2	1.09	2363	0.440
72	1766	1620	65.0	2.20	3014	0.593	16	735	651	24.8	1.09	2330	0.436
71	1746	1601	64.5	2.20	2992	0.591	15	722	639	24.5	1.09	2297	0.432
70	1725	1583	64.0	2.20	2969	0.589	14	709	626	24.1	1.09	2263	0.428
69	1713	1572	62.1	2.06	3077	0.596	13	687	606	23.8	1.09	2230	0.429
68	1695	1555	61.7	2.06	3056	0.595	12	673	594	23.4	1.09	2195	0.424
67	1676	1538	61.3	2.06	3035	0.593	11	660	581	23.0	1.09	2160	0.420
66	1657	1521	60.8	2.06	3013	0.591	10	647	569	22.6	1.09	2124	0.415
65	1639	1503	60.4	2.06	2991	0.589	9	634	556	22.3	1.09	2088	0.410
64	1620	1486	59.9	2.06	2969	0.587	8	620	544	21.9	1.09	2051	0.404
63	1602	1469	59.5	2.06	2947	0.585	7	607	531	21.5	1.09	2013	0.399
62	1582	1451	56.9	1.90	3047	0.586	6	569	496	20.8	1.10	1922	0.396
61	1565	1436	56.5	1.90	3026	0.584	5	558	486	20.5	1.10	1893	0.391
60	1548	1420	56.1	1.90	3005	0.582	4	548	477	20.2	1.10	1863	0.386
59	1531	1404	55.7	1.90	2983	0.580	3	538	467	19.8	1.10	1832	0.382
58	1514	1388	55.3	1.90	2962	0.579	2	527	457	19.5	1.10	1801	0.377
57	1498	1372	54.9	1.90	2940	0.577	1	517	448	19.2	1.10	1770	0.371
56	1481	1357	54.5	1.90	2918	0.575	0	507	438	18.8	1.10	1738	0.366

Table 4. FT3 Initial Checkout Results.

FT3 Initial Checkout															
		Beam		Accel.		Discharge			Neutralizer		PPU			REQUIRED	
Mission Level		J_B	V_B	J_A	V_A	J_D	V_D	Discharge Loss	J_{NK}	V_{NK}	Input Power	Efficiency	Dissipated Power	Main Plenum	Cath Plenum
		(A)	(V)	(mA)	(mA)	(A)	(V)	(eV/ion)	(A)	(A)	(W)		(W)	(psia)	(psia)
27	Expected	0.610	1100	0.83	-200	5.44	26.7	239	2.4	15.6	984	0.907	89	18.69	23.50
	Actual	0.606	1100	0.83	-200	5.38	26.3	233	2.4	16.8	935	0.908	86	18.80	23.50
48	Expected	0.910	1100	1.57	-200	7.39	25.4	207	2.3	14.7	1340	0.920	104	30.95	23.50
	Actual	0.907	1100	1.54	-200	7.38	25.4	207	2.3	15.4	1329	0.919	108	31.30	23.50
69	Expected	1.200	1100	2.79	-200	8.87	25.0	185	2.0	14.5	1713	0.923	132	44.44	23.50
	Actual	1.197	1100	2.44	-200	8.89	25.2	187	2.0	14.8	1694	0.927	123	44.70	23.50
90	Expected	1.490	1100	4.12	-200	10.55	25.1	178	1.7	14.1	2105	0.923	162	56.21	27.30
	Actual	1.487	1100	3.54	-200	10.69	25.6	184	1.7	14.3	2073	0.933	138	56.40	27.30
111	Expected	1.760	1100	5.63	-200	12.99	24.4	180	1.5	13.9	2483	0.924	189	67.35	35.04
	Actual	1.756	1100	4.59	-200	13.09	25.0	186	1.5	13.9	2435	0.937	154	67.30	35.00

Table 5. FT1 Initial Checkout Results.

FT1 Initial Checkout															
		Beam		Accel.		Discharge			Neutralizer		PPU			REQUIRED	
Mission Level		J_B	V_B	J_A	V_A	J_D	V_D	Discharge Loss	J_{NK}	V_{NK}	Input Power	Efficiency	Dissipated Power	Main Plenum	Cath Plenum
		(A)	(V)	(mA)	(mA)	(A)	(V)	(eV/ion)	(A)	(A)	(W)		(W)	(psia)	(psia)
27	Expected	0.610	1100	1.50	-200	6.00	27.6	271	2.4	16.5	984	0.907	89	18.19	23.47
	Actual	0.605	1100	0.81	-200	5.84	27.1	262	2.4	16.2	936	0.922	73	18.21	23.51
48	Expected	0.910	1100	2.67	-200	7.88	26.3	228	2.3	15.3	1340	0.920	104	29.86	23.47
	Actual	0.907	1100	1.59	-200	7.79	26.2	225	2.3	14.9	1320	0.936	84	29.87	23.51
69	Expected	1.200	1100	3.87	-200	9.37	25.8	201	2.0	14.7	1713	0.923	132	42.62	23.47
	Actual	1.197	1100	2.53	-200	8.99	25.9	195	2.0	14.2	1685	0.937	107	42.63	23.51
90	Expected	1.490	1100	5.10	-200	11.24	25.7	194	1.7	14.2	2105	0.923	162	53.70	27.27
	Actual	1.487	1100	3.63	-200	11.25	26.0	197	1.7	13.7	2075	0.941	123	53.69	27.30
111	Expected	1.760	1100	6.42	-200	13.94	24.6	195	1.5	13.9	2483	0.924	189	64.19	35.01
	Actual	1.756	1100	4.84	-200	14.00	24.9	199	1.5	13.5	2458	0.936	156	64.21	35.09

Table 5. FT2 Initial Checkout Results

FT2 Initial Checkout															
		Beam		Accel.		Discharge			Neutralizer		PPU			REQUIRED	
Mission Level		J_B	V_B	J_A	V_A	J_D	V_D	Discharge Loss	J_{NK}	V_{NK}	Input Power	Efficiency	Dissipated Power	Main Plenum	Cath Plenum
		(A)	(V)	(mA)	(mA)	(A)	(V)	(eV/ion)	(A)	(A)	(W)		(W)	(psia)	(psia)
27	Expected	0.610	1100	1.57	-200	5.37	26.6	234	2.4	15.4	938	0.907	87	18.20	24.63
	Actual	0.606	1099	0.86	-200	5.54	26.2	240	2.4	16.5	948	0.898	97	18.41	24.85
48	Expected	0.910	1100	2.74	-200	7.34	25.3	204	2.3	14.5	1327	0.920	106	30.06	24.63
	Actual	0.907	1099	1.63	-200	7.65	25.0	211	2.3	15.1	1341	0.912	118	30.32	24.85
69	Expected	1.200	1100	3.97	-200	8.89	24.8	184	2.0	14.2	1701	0.923	131	43.15	24.63
	Actual	1.197	1099	2.63	-200	9.20	25.0	192	2.0	14.6	1711	0.921	136	43.49	24.85
90	Expected	1.490	1100	5.21	-200	10.70	24.9	179	1.7	13.9	2091	0.923	161	54.56	28.64
	Actual	N/A	N/A	N/A	N/A	N/A	N/A	N/A	N/A	N/A	N/A	N/A	N/A	N/A	N/A
111	Expected	1.760	1100	6.59	-200	13.22	23.9	180	1.5	13.7	2461	0.924	187	65.32	36.78
	Actual	1.756	1098	4.67	-200	13.46	24.2	185	1.5	12.0	2454	0.926	181	65.67	37.09

Table 7. In-flight Measured Thrust Levels Compared to Pre-flight Expected Values

Throttle Level	Input Power (W)		FT1 Thrust (mN)	FT2 Thrust (mN)	FT3 Thrust (mN)
ML27	940	Expected	31.4 ± 1.37	31.4 ± 1.37	31.4 ± 1.37
		Actual	31.69 ± 0.10	31.63 ± 0.09	31.59 ± 0.02
ML48	1320	Expected	47.1 ± 1.36	47.1 ± 1.37	47.1 ± 1.38
		Actual	47.13 ± 0.13	47.21 ± 0.13	47.04 ± 0.02
ML69	1685	Expected	62.1 ± 1.36	62.1 ± 1.37	62.1 ± 1.38
		Actual	62.06 ± 0.17	62.15 ± 0.18	62.02 ± 0.03
ML90	2075	Expected	76.7 ± 1.45	76.7 ± 1.46	76.7 ± 1.47
		Actual	76.95 ± 0.21	N/A	76.91 ± 0.04
ML111	2460	Expected	91.0 ± 1.65	91.0 ± 1.66	91.0 ± 1.67
		Actual	91.43 ± 0.23	91.72 ± 0.52	91.30 ± 0.07

Table 8. Double-to-Single Ion Currents.

Mission Level	Centerline Values	Slice Values	Combined Total	
	J++/J+	J++/J+	J++/J+	α
ML111	0.262	0.150 ± 0.018	0.091 ± 0.011	0.976
ML90	0.295	0.182 ± 0.011	0.103 ± 0.013	0.973
ML69	0.245	0.144 ± 0.008	0.077 ± 0.007	0.979
ML48	0.191	0.121 ± 0.011	0.068 ± 0.009	0.981
ML27	0.127	0.090 ± 0.017	0.058 ± 0.017	0.984
ML6	0.060	0.039 ± 0.005	0.022 ± 0.005	0.994